Targeting Microhabitats in Ice For Life Detection

KISS Workshop Study Report, March 2025

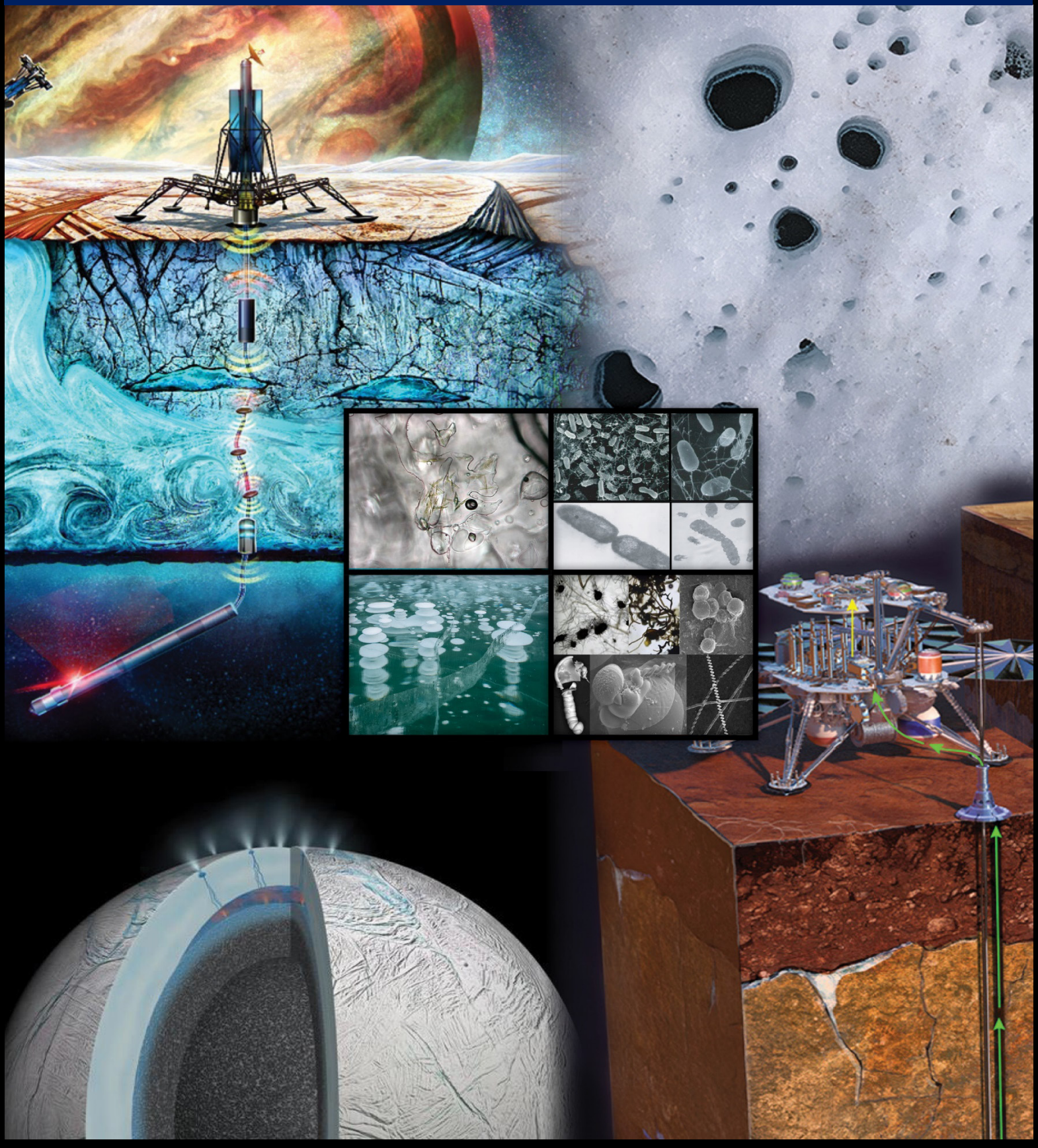

Keck INSTITUTE FOR SPACE STUDIES

Date: March 2025

Study Workshop 1: September 19-23, 2022

Study Workshop 2: March 27-31, 2023

Study Leads

Heather Graham
NASA Goddard Space Flight Center
heather.v.graham@nasa.gov

Charity Phillips-Lander
SWRI
charity.lander@swri.org

Jeff Marlow
Boston University
jjmarlow@bu.edu

Michael Malaska
Jet Propulsion Laboratory, California Institute of Technology
michael.j.malaska@jpl.nasa.gov

Study Report prepared for the W. M. Keck Institute for Space Studies (KISS)

A portion of this research was carried out in part at the Jet Propulsion Laboratory, California Institute of Technology, under a contract with the National Aeronautics and Space Administration (80NM0018D0004).

Pre-Decisional Information — For Planning and Discussion Purposes Only

DOI: 10.26206/mfmfk-2ys71

Recommended citation (long form):

D. Anthony, M. Badescu, J. Buffo, E. Cardarelli, K. Carpenter, B. Carrier, H. Graham, L. Hays, J. Huber, B. Hug, N. Johnston, S. Lamm, J. Lawrence, M. Malaska, J. Marlow, B. Mellerowicz, J. Nadeau, A. Noell, N. Oborny, V. Orphan, C. Parker, C. Phillips-Lander, P. Sobron, A. Stockton, L Stolov, J. Wekselblatt, M. Wilhelm, C. Williamson, D. Winebrenner, C. Yang, K. Zacny, O. Zhang 2025. "Targeting Microhabitats in Ice For Life Detection" H. Graham, C. Phillips-Lander, J. Marlow, M. Malaska (Eds.) Report prepared for the W. M. Keck Institute of Space Studies (KISS), California Institute of Technology.

Recommended citation (short form):

H. Graham, C. Phillips-Lander, J. Marlow, M. Malaska (Eds.). 2025. "Targeting Microhabitats in Ice For Life Detection" Report prepared for the W. M. Keck Institute of Space Studies (KISS), California Institute of Technology.

Acknowledgements

Prof Bethany Ehlmann
Director

Harriet Brettle
Executive Director

Janel Wilsey
Editing and Formatting

Cover Image:
Cover Image - Upper left: NASA/JPL-Caltech, upper right: Mike Malaska, lower left: NASA, lower right: Chuck Carter / Keck Institute for Space Studies, middle-upper left and right: NOAA, middle-lower left: Jeff Wallace CC BY-NC 2.0, middle-lower right: McMahon & Cosmidis/Journal of the Geological Society

We gratefully acknowledge both the financial and organizational support of the Keck Institute for Space Studies, without which this study would not have been possible. This included support for two graduate students and three postdoctoral scholars.

Workshop Participants

David Anthony - Southwest Research Institute (SwRI)	Mircea Badescu - JPL
Jacob Buffo - Dartmouth College**	Emily Cardarelli - JPL
Kalind Carpenter - Manakin	Brandi Carrier - JPL **
Heather Graham - NASA Goddard Space Flight Center	Lindsay Hays - NASA Headquarters
Julie Huber - Woods Hole Oceanographic Institution (WHOI) *	Bill Hug - Photon Systems, Inc.*
Nikki Johnston - Portland State University*	Sarah Lamm - University of Kansas
Justin Lawrence - Honeybee Robotics	Michael Malaska - JPL
Jeff Marlow - Boston University	Bolek Mellerowicz - Honeybee Robotics*
Jay Nadeau - Portland State University*	Aaron Noell - JPL
Nathan Oborny - JPL**	Victoria Orphan - Caltech
Ceth Parker - JPL	Charity Phillips-Lander - Southwest Research Institute (SwRI)
Pablo Sobron - Impossible Sensing	Amanda Stockton - Georgia Institute of Technology**
Leo Stolov - Honeybee Robotics**	Joe Wekselblatt - Caltech**
Mary Beth Wilhelm - NASA Ames Research Center*	Chris Williamson - University of Bristol**
Dale Winebrenner - University of Washington	Changhuei Yang - Caltech*
Kris Zacny - Honeybee Robotics*	Oumeng Zhang - Caltech**

* Attended 1st workshop only

** Attended 2nd workshop only

Executive Summary

The search for life on other worlds is one of the most significant drivers of scientific exploration. On Earth, microbial life inhabits tiny places on a scale of hundreds of microns across or even smaller. These microhabitats and niches have favorable physical conditions and chemical disequilibria, enabling life to survive and thrive locally. For example, in the Greenland Ice Sheet, ultrasmall microbes live under cold, dark, high-pressure conditions found kilometers below the surface (Miteva and Brenchley 2005). In the deep ice, microbes survive in hypersaline liquid micro-pockets located between ice grains (Price 2000, Junge, Krembs et al. 2001, Junge, Eicken et al. 2004, Mader, Pettitt et al. 2006, Barletta, Pricsu et al. 2012). Since terrestrial deep ice microhabitats may have similar physical and chemical conditions as those deep locations in the icy crusts of the Ocean Worlds of the Solar System, such as Europa, Enceladus, and Titan Titan (Priscu and Hand 2012, Vance, Panning et al. 2018), it is possible that those alien microenvironments are inhabited and thus are excellent targets in the search for life.

Unfortunately, current techniques for looking and sampling for life on other worlds operate at the bulk scale, on the order of 1 cm^3 (1E–6 m^3) or larger (Hand, Murray et al. 2016) Lander Study report. The current paradigm for identifying extraterrestrial biosignatures involves multiple approaches, including detecting distinctive chemical signatures, looking for likely morphologies, and measuring for metabolic activity. Compared to current strategies involving large-scale bulk sampling, targeting microenvironments will improve the signal-to-noise for each approach. This is because specifically targeting the microenvironments leads to the acquisition of less of the surrounding matrix (e.g., ice), which in turn means that the resulting chemical and biological signals are less diluted. The resulting increase in signal strength could be up to two orders of magnitude (Malaska, Bhartia et al. 2020). In a nutrient-starved environment, such as those predicted for the Ocean Worlds (Affholder, Guyot et al. 2022, Neish, Malaska et al. 2024), this signal increase could translate to the difference between detection and non-detection of key biosignatures. In addition, by specifically targeting the individual microenvironments, any detected signals can be placed within the local chemical context without comingling of surrounding matrix. By developing technologies to target, extract, and analyze the contents and context of potentially inhabited alien microenvironments, we will significantly advance our search for life in alien environments.

Our KISS study identified techniques and technologies for instrumentation and robotics to be able to identify, target, sample, and analyze microenvironments in Ocean World environments and also the surface of ice-rich areas on Mars. Implementation of these requirements could enhance capabilities for future astrobiological exploration Mars and the Ocean Worlds during in situ surface or subsurface missions.

The following themes, topics, and notes emerged as our study's key findings and recommendations:

The current astrobiology paradigm is shifting away from biosignature detection and toward understanding the biosignature signal within its surrounding context—context that will be lost

during commingling associated with 'bulk' sampling. Small-scale targeting and analysis of microenvironments that may exist on Ocean Worlds enables the original biosignature concentrations and contextual signals to be preserved. By making these investments and developing microhabitat technologies, we significantly improve our astrobiological exploration of the Ocean Worlds and frozen surfaces and subsurfaces.

On Ocean Worlds, which are large enough to host convection in their ice shell(s), there may be large regions of the ice shell that could support active metabolism. For example, the temperature and pressure conditions at the top of the convective zone in Europa's and Titan's ice shells correspond to the temperature and pressure at the base of the Greenland ice sheet (Vance, Panning et al. 2018). At this terrestrial location, a diverse array of ultrasmall microbes have been found (Miteva and Brenchley 2005). These microbes live in 10–100 micron diameter hypersaline micropockets between frozen ice grains (Price 2000, Junge, Krembs et al. 2001, Junge, Eicken et al. 2004, Mader, Pettitt et al. 2006, Barletta, Pricsu et al. 2012). During freezing, impurities such as salts and some organics present in the water are rejected by the growing water ice crystals, leading to chemically concentrated hypersaline liquid micropocket between the ice grains. For some ions, this concentration effect can be up to 5 orders of magnitude (Barletta, Pricsu et al. 2012). This natural concentration effect creates an ideal environment enriched in nutrients for any microbial inhabitants. The same physical and chemical principles occur on ices across the Solar System, creating chemically concentrated microenvironments that may be inhabited by alien life.

We recommend adapting current analytical instrumentation and techniques for small sample volumes in the microliter to nanoliter range for detailed astrobiological analysis of microhabitats. Because of the concentration effect of microhabitats and ROIs, instrument sensitivity requirements (i.e., limits of detection and/or quantitation) are likely already met. Techniques such as capillary electrophoresis (CE), Raman, or (non-rastering) mass spectrometry or even microscale metabolic tests would all be good investments. In short, we recommend investments to adapt the compendium of "life" tests (i.e., chirality, morphology, isotopes) recommended by the astrobiology community to use 1–2 microliters to nanoliters of total sample volume.

For initial detecting ROIs and microhabitats, we recommend investment in developing and ruggedizing a DUV fluorescence/optical imaging system. The ideal instrument would be able to scan a wide field of view using fluorescence detection at 100 microns per pixel scale with optical context imaging at 30 microns per pixel. The ability to zoom into features of interest to characterize the target features and surrounding context before extraction would be advantageous.

We recommend investing in developing epifluorescence-staining techniques for in situ biosignature investigation. Developing the technology to stain with multiple agents would augment the fluorescence instrument above and provide additional chemical information such as metabolic transformation, incorporation into a nucleus, etc. This could also enhance post-sample acquisition fluorescence analysis so that this technology could provide chemical information before and after sample acquisition.

A high-risk but high-reward approach would be to study technology paths to develop a rastering mass spectrometry-based system for flight. Combined with an optical/fluorescent instrument above, a rastering mass spectrometer would give a powerful synergistic combination of data for target features before acquisition. (The power would exceed the synergies observed with SHERLOC/PIXL). In such a combination, we would have information on electronic transitions and elemental combinations that would narrow and refine possible structures or functionalities.

We recommend the development of information-transfer, automated decision-making, and robotics technologies to detect, prioritize autonomously, and target microhabitats for extraction given an initial instrument image. This includes developing precision targeting and extraction techniques from Ocean World matrices of ice, ice/sediment, sediment, and solid rock combinations to relevant depths. Extraction can be either as a microcore, commingled drilled material, or meltwater in the case of ice.

We also recommend carrying out further in situ exploration of ocean-world-like terrestrial environments: ocean ice, ice sheets, deep-sea sediments, ocean-ice interface, rock-air interface, in situ deep ice (drilling), deep rock (drilling) to not only test and assess the performance of instrumentation and techniques, but also to acquire additional information on terrestrial microhabitats, which can help guide all the endeavors listed above.

Table of Contents

Table of Figures

Table of Tables

1. Introduction

1.1 The need to think small—Life inhabits tiny places.

Our current techniques for looking and sampling for life on other worlds operate at "bulk" scales on the order of 1 cm^3 or larger. State-of-the-art planetary instrumentation is based on bulk scale sampling larger than the microenvironments life inhabits (Fig. 2.) (Hand, Murray et al. 2016).

However, recent work examining microorganisms in native substrates on Earth shows that life's metabolic opportunities (Marlow, Spietz et al. 2021) and long-term stability are dictated by much smaller environments: between the ice grains (**Figure 1**) between sediment grains, or inside rock vesicles, with some environments as small as 1E–15 m^3 (Junge, Krembs et al. 2001). These microenvironments can be chemically distinct and host divergent microbial communities (Barletta, Pricsu et al. 2012).

The microbial "sphere of influence" within complex communities can be as small as a few microns, revealing the importance of microscale spatial arrangements when considering microbe-microbe and microbe-mineral interactions (Dal Co, van Vliet et al. 2020, van Gestel, Bareia et al. 2021). Interpretation and understanding of the importance of a biological signal are critical to understanding the quality of this evidence for any alien biosignature (Dal Co, van Vliet et al. 2020, van Gestel, Bareia et al. 2021), and the confidence of an interpretation relies on exquisite fine-scale characterization.

With bulk-scale sampling, this spatial context in microenvironments is lost, diverse microenvironments become mixed together, and information-rich gradients are obscured. In addition, explicitly targeting discrete microenvironments reduces the dilution of diagnostic chemical and biological signals by the surrounding matrix (e.g., ice). The resulting increase in signal strength could be up to two orders of magnitude (Malaska, Bhartia et al. 2020).

In a nutrient-starved environment, such as those predicted for the Ocean Worlds (Affholder, Guyot et al. 2022, Neish, Malaska et al. 2024), this signal increase could mean the difference between detection and non-detection of key biosignatures. As we explore potentially habitable niches beyond Earth, analyzing and sampling at the microenvironment scale while retaining precise spatial arrangements enables the best chance of transformational discovery in the search for evidence of life elsewhere.

Targeting microhabitats will be a paradigm shift in the community's approach to astrobiological exploration and the design of instrumentation and sampling technologies.

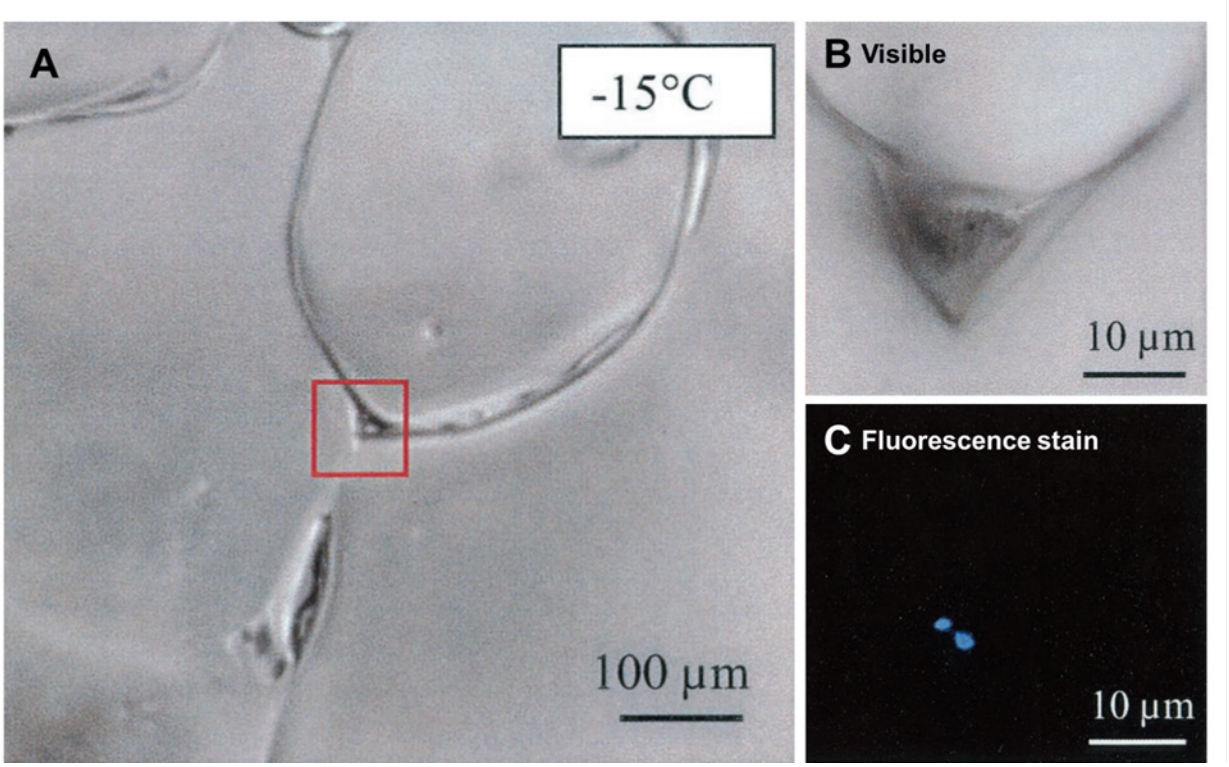

Figure 1. Ice microenvironments. **(A)** Visible light image of a hypersaline liquid pocket existing at a triple junction between sea ice grains (red box). **(B)** Detailed image of the same pocket in (A) under visible light. The micropocket is roughly 10 microns across. **(C)** Fluorescence imaging of a detailed view of the same micropocket in B reveals two microbes localized in the pocket. Images from Junge et al., 2004, and used with permission of author.

1.2 Importance of Microhabitats on Earth and for the Search for Life Elsewhere

In recent decades, three parallel trends in microbiology, planetary science, and engineering have emerged to reconfigure our search for life beyond Earth. Continued exploration of Earth's microbial biosphere has yielded discoveries of habitats and organisms that have transformed our understanding of the limits of life: microbes surviving kilometers deep in the Earth's crust (Inagaki, Hinrichs et al. 2015) in hypersaline basins (Van Der Wielen, Bolhuis et al. 2005), and in thin films of liquid between ice crystals (Deming 2007) have shown the remarkable adaptability and metabolic ingenuity of microbial communities. In parallel, a better understanding of extreme habitats on Earth and measured or predicted conditions similar to those on other worlds in our solar system have expanded the range of potential habitats and environments for future exploration.

At the same time, technological advances, particularly around precision mechanical manipulation, microfluidic analysis, and non-destructive sensing techniques, have enabled the characterization of tiny sample volumes. As we observe the confluence of these three rapidly developing fields, there is a renewed sense of urgency and excitement around the search for extant life beyond Earth. With further exploration of subsurface icy and endolithic environments on Earth and missions concepts in development to explore the deep icy crusts

and oceans of Europa and Enceladus, as well as the surface and subsurface of Mars, the next decade promises to be a critical time for technology development for the search for life in extreme environments and extraterrestrial life.

The most likely form of extant life in our Solar System is microbial (e.g., single-celled organisms with relatively simple internal structure). Microbial life was the first to evolve on Earth and has dominated the biosphere ever since, with the relatively recent evolution of more 'complex' life only made possible through a series of microbially mediated transformations of Earth's (bio)geochemistry.

Although small—generally invisible to the unaided eye—microbes are ubiquitous and abundant, thanks mainly to their ability to evolve as the Earth has passed through various environmental states. Today, the organisms considered the best analogs for extraterrestrial life are represented by microbial communities that thrive under extreme temperature, salinity, pH, and pressure within environments that remain microbially dominated.

Microbial "neighborhoods"—the volumes in which microbes interact with their biotic and abiotic surroundings occur at the microscale. One study of microbial cultures showed a preferential interaction distance of just tens of microns (Dal Co, van Vliet et al. 2020), while another demonstrated cell-cell communication through quorum sensing restricted to just a few microns (van Gestel, Bareia et al. 2021). Stark concentration gradients in metabolites (van Tatenhove-Pel, Rijavec et al. 2020) or geochemical energy sources—gradients that the microbes may generate (Smriga, Ciccarese et al. 2021) also operate across tens of microns.

While a microbe's interaction distance can expand beyond these small scales, particularly in fluid environments with high advection rates, most microbial life hosted in sediment, soil, and rock pores has a sub-mm "sphere of influence." In this context, the notion of the "microhabitat" serves as a useful structuring framework for understanding microbial life on its own terms. We define a microhabitat as a discrete habitable volume (on the ~sub–mm scale) within a larger physical or chemical matrix.

These microhabitats, which include such chemically distinct settings as hypersaline brines between ice grains, sediment pore spaces, or rock vesicles, can differ substantially from the bulk composition of the wider environment. They may concentrate biochemical resources and energy sources and provide protection from unfavorable conditions. The concentrating effects of microenvironments extend to biological and chemical signals compared to the bulk environment and can provide enhanced signals compared to the bulk matrix. Microhabitats that sustain life under extreme conditions are thus high-priority targets for life detection on other worlds.

Since microbial communities operate at the microscale, they can produce global impacts, and even while a focus on microhabitats may provide the best chance of extant life detection, interpretive power is bolstered with simultaneous bulk sampling. Understanding the geologic, climatic, geochemical, and biological processes that occur during microhabitats' formation, maintenance, and alteration will provide essential information about habitability. In other words, the distinct characteristics of habitable microhabitats are informed by comparison with

their bulk surroundings. Such multidimensional analytical approaches will be central to the search for life on other planetary bodies.

Numerous community workshops have been convened to address the best way to detect life, extant or otherwise, on bodies elsewhere in our Solar System. A growing consensus among astrobiologists is that a combination of tests involving chemical, morphological, and activity-based measurements will provide the best chance of accumulating sufficient evidence required to convince the scientific community and general public alike that life has been found.

While this framework is a robust starting point, it undervalues the importance of micro-scale measurements that provide direct context with respect to the surrounding environment. Demonstrating that local variables (e.g., pH, specific ions, or the co-localization of organic molecules) are consistent with the specific biosignature measurements is the true power of these contextual measurements. Fundamentally, we contend that missions should thus strive to perform analyses at the micro-scale—where any extant extraterrestrial life is most likely to operate.

This proposed approach raises a critical challenge for life detection missions, as existing technologies to examine and sample for life in both icy and soil-dominated environments are typically designed to operate at "bulk" scales on the order of 1 cm^3 or larger, where key signals could be diluted or confounded so that detection is challenging.

This workshop focused on considering the strategic value of a microhabitat-centric perspective while also evaluating the existing technologies that could be used to study microhabitats on Earth and other planetary bodies. We provide recommendations about the future scientific, analytical, and robotic developments required to develop our understanding of life in microhabitats on Earth and how we can leverage these efforts to search for life elsewhere.

2. The KISS Microhabitats Workshop

2.1 Study Goal

The goal of our study was to 1) consider relevant analog examples of microhabitats and evaluate the utility of the microhabitat concept as an organizing principle for astrobiological exploration and 2) survey existing microhabitat sampling options and develop an in situ exploration strategy for life detection in microhabitats.

2.2 Study Process

This study was organized through the Keck Institute for Space Studies on the California Institute of Technology campus in Pasadena, CA. Participants were selected based on their astrobiology, planetary geology, microbiology, geology and geobiology, instrumentation, and robotics expertise. The study was held over two one-week periods in September 2022 and March 2023. During each week, participants worked in several large group sessions to examine critical points for detailed evaluation in smaller groups. These small group breakout sessions discussed these points to inform the results below.

3. Microhabitats on Earth

We define a microhabitat as a discrete habitable volume (on the ~sub-mm scale) within a larger physical or chemical matrix. A wide array of microhabitats exists within the terrestrial critical zone (encompassing the cryosphere and shallow lithosphere), which support a diverse community of microorganisms that thrive in these discrete, confined systems. Many of these microbial residents exploit and rely upon the unique physical traits, thermophysical properties, and geochemical gradients these substructures offer; some microbes actively modify their environment, which may support their metabolic needs.

For example, seawater freezes to produce sea ice. This process concentrates salts and microbial cells within brine inclusions that provide a tight spatial association between primary and secondary producers, a higher concentration of labile organic matter, and lower grazing pressures (Cooper, Rapp et al. 2019, Rapp, Sullivan et al. 2021). As a result, microbial communities can establish feedbacks that regulate microhabitats to their favor through, for example, the production of ice-binding proteins that regulate ice crystal growth and increase and maintain the habitable space (Deming 2009).

Here, we summarize a range of terrestrial analog environments relevant to the putative planetary microhabitats and outline the thermophysical and biogeochemical properties of such systems that control their habitability. We further highlight empirical techniques to characterize terrestrial microhabitats and quantify their biological potential/properties/productivity/density.

3.1 Terrestrial Analogs of Ocean Worlds

Terrestrial systems most pertinent to the icy shells of moons like Europa, Enceladus, Triton, and Titan include sea ice, lake ice, ice shelves, marine ice, and ice sheets. Sea ice and lake ice form via conductive heat loss and solidification of the underlying reservoir at propagating ice-ocean/lake interfaces. As this interface grows, it entrains fluid-derived solutes and organisms. Regions of the ice cover that remain above the eutectic freeze-out temperature of the parent reservoir (the point at which the entire system solidifies as either ice or salt hydrates) will contain some liquid fraction in the form of highly concentrated brine pockets/channels and along grain boundaries/triple junctions (Figure 2 **left**). From Barletta et al., Journal of Glaciology, 2012; GISP2 ice core from 146 m depth. vein fluid in zones a, b, and c exhibited enrichments of 200000 and 400000 in sulfate and nitrate concentrations, respectively, compared with bulk snow composition.

This concentration mechanism is due to the freezing point depression of dissolved species, which can lower the freezing point by as much as 20 K or more, depending on the solute. Because small particles in freezing fluids are partitioned into the remaining liquid phase (Figure 2 right*), the concentration of microbes in these residual liquid regions is drastically higher than in the background ice matrix. It is often higher than that of the underlying fluid. These fluid-saturated, porous ice matrices protect microbes from larger grazers and support significant thermochemical gradients and fluid recharge within the connected channel networks that can be leveraged to support and maintain metabolic processes. Several microbial

species can produce extracellular polymeric substances (EPS) that modify local ice geometry for improved fitness.

If the temperature drops below the eutectic temperature, brine veins and channels freeze out as eutectic solids and/or salt hydrates (Carns, Brandt et al. 2015). Salt hydrates' biological preservation potential provides long-term advantages to organisms colonizing these microhabitats even during times of environmental stress. Understanding the distribution and coevolution of organisms within these diverse analog systems can help inform search-and-sampling techniques for missions exploring planetary ices.

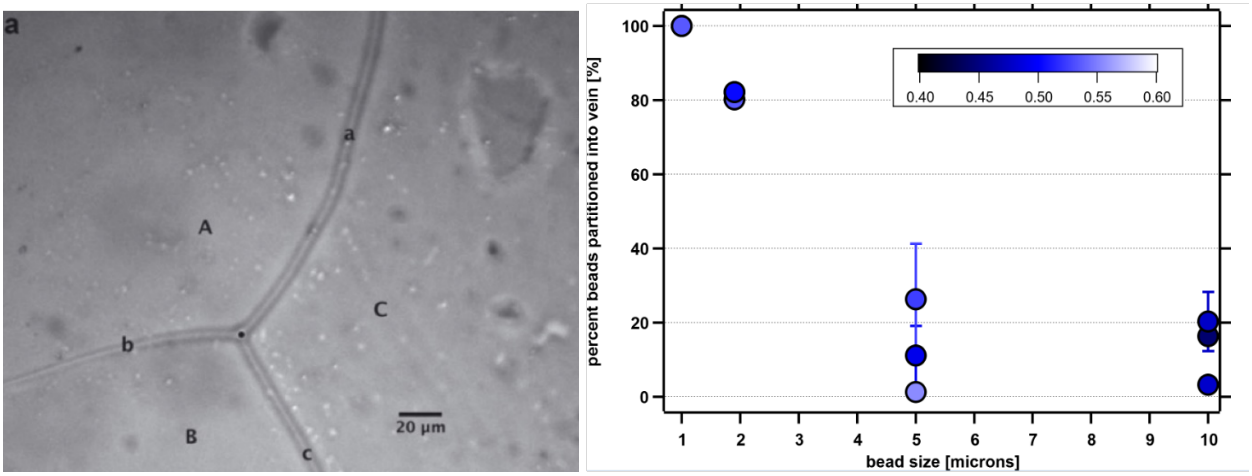

Figure 2. (left) Image of triple junction of GISP2 ice core from 146 m depth showing the location of increased chemical concentration due to partitioning and exclusion during ice crystallization. GISP2 ice core from 146 m depth. Veins exhibited enrichments of 200000 and 400000 in sulfate and nitrate concentrations, respectively, compared with bulk composition. Image from (Barletta, Pricsu et al. 2012) and used with permission of the author (right) plot using data from (Mader, Pettitt et al. 2006) showing the percentage of insoluble beads that are partitioned into the liquid ice vein during freezing. Beads larger than 5 microns become entombed in the ice. Ice veins favor insoluble materials that are less than 5 microns.

3.1.1 Marine Ice as an Analog for the Base of Ocean World Ice Shells

Marine ice forms at the base of floating ice shelves via an inverted ice crystal deposition process known as the ice pump (Lewis and Perkin 1986). The deposition and buoyancy-driven compaction of these fresh ice crystals leads to ice with a bulk composition that is typically lower in solute, gas, and organic concentrations than sea ice.

The purity and isolated nature of this ice provide an analog that may have physical and chemical signals more similar to ice grown under the low thermal gradients at the base of planetary ice shells—offering a novel opportunity to test microhabitat identification as well as instrument sampling techniques and detection limits in an oligotrophic environment. Porous marine ice warmer than the eutectic temperature likely contains a nonzero liquid fraction. Marine ice can also be permeable (Craven, Allison et al. 2009).

In these liquid pockets, organics, minerals, and single-celled life can concentrate. The difficulty in accessing marine ice environments means a limited amount of data is available about the

physicochemical nature of this ice type (a comprehensive review can be found in (Wolfenbarger, Buffo et al. 2022). As a unique analog for planetary ice shells and a byproduct of ice shelf mass balance, continued research on and understanding marine ice layers is pertinent to planetary and Earth/climate science communities.

3.1.2 Meteoric Ice as an Analog for Accessing Ocean World Ice Shells

Meteoric ice represents ice formed via the deposition and compaction of snow. While not generated by the solidification of an ocean, meteoric ice provides a broad spectrum of material, age, and biological properties to investigate the diversity of ice microhabitats and test engineering concepts for future planetary environments.

Viable organisms have been found at all depths within meteoric ice sheets. Populating gas—and liquid—filled pore spaces above the clathrate horizon (the depth at which pressure forces gas into the ice lattice, significantly reducing the ice's porosity) as well as grain boundaries below this layer, these deep ice environments provide a unique resource to understand long-term preservation and sampling techniques for organisms in cryogenic environments.

3.1.3 Terrestrial Analogs for Martian Permafrost

Recent work has shown that Mars hosts modern glacial features (Lee, Shubham et al. 2023) as well as permafrost features like patterned ground and recurring slope lineae (Ojha, Wilhelm et al. 2015, Khuller, Kerber et al. 2023). Computational modeling suggests that significant water ice is present in the Mars subsurface; in one recent impact crater, this subsurface ice was exposed to the atmosphere before sublimating (Dundas, Mellon et al. 2023). Based on these observations, Earth's permafrost systems represent subterranean Mars' potential analogs. Permafrost is defined as ground that remains at or below 273 K for at least two consecutive years; its depth beneath the surface depends on the mean air temperature and local geothermal gradient and thus may be spatially variable. Even in the same region, ice fill in subsurface soils can range from 0–100% ice (i.e., pore-filling ice to massive ice lenses) across a landscape.

The layer of soil above the permafrost that freezes and thaws annually is called the active layer. This additional lithologic phase increases the thermophysical and biogeochemical complexity of analogous terrestrial systems and the microhabitats that they house. In particular, phase interfaces between ices, brines, rocks, and sediments provide ample geochemical resources and substrates essential for maintaining cellular functions. Biological materials in permafrost and massive ground ice on Earth concentrate along pores, grain boundaries, and—most prominently—non-ice impurities such as mineral grains.

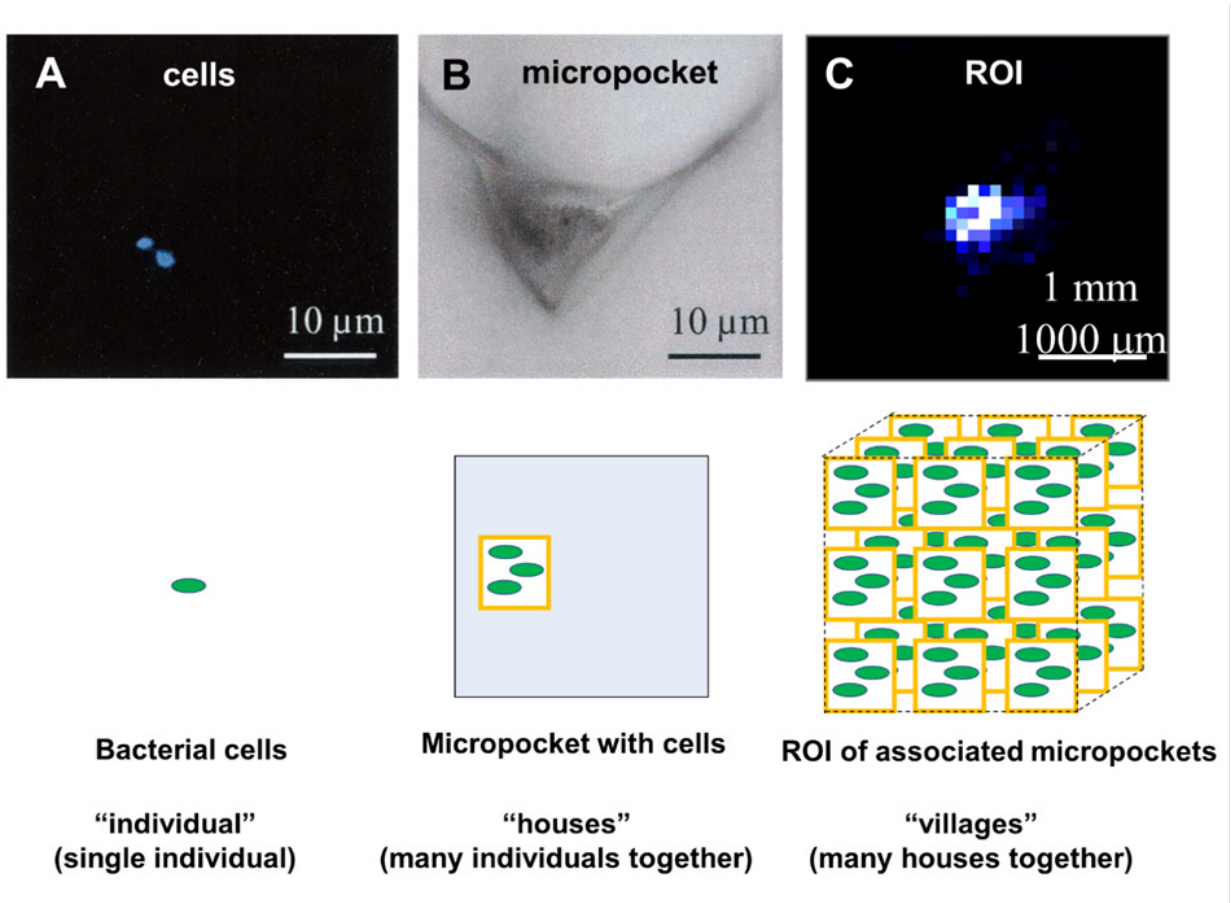

Figure 3. Example images of features of each type. **A:** cells in the micropocket in panel 6b indicated by DAPI staining epifluorescence (image adapted from (Junge, Eicken et al. 2004), Fig. 1b in text and used with permission of the author). **B:** micropocket in sea ice imaged by oil immersion visual microscope (image adapted from (Junge, Eicken et al. 2004), Fig. 1b in text and used with permission of the author). **C:** ROI in glacial ice in situ at 93.8 in Greenland ice sheet imaged by Deep-UV fluorescence (graphic adapted from (Malaska, Bhartia et al. 2020), Fig. 10a in text and used with permission of the author). The lower section of the graphic shows the relationship between individuals, micropockets, and ROIs.

Table 1. Table of averaged characteristics for each feature type.

	Average measured spatial area [microns^2]	Average measured maximum length [microns]	Average distance between features [microns]	Average number of cells [cells][a]	Average estimated spherical volume [microns^3]
ROI	1.74E6	1255	1880	2105	1.03E9
micropocket	2894	92	120	9	4.10E5
bacterial cell	17.8	3.8	17.7	1	1.8

a. average is based on a numerical average of all entries weighted equally.

4. Current Sampling Strategies

Bulk sampling has been the primary method for planetary exploration, in which relatively large volumes of material are collected and analyzed as a single unit. Scientists conventionally use quantitative environmental analytical techniques on bulk materials; however, several technologies exist in the medical and environmental fields for small-scale, precision sample analysis in spatial contexts*.

These microanalytical approaches uniquely reveal heterogeneity within ice and rock samples, providing critical context for the local biological, physical, and chemical environment. Despite these potential advantages, researchers must weigh the relative strengths and weaknesses of sampling and analyzing materials from different environments at different scales. Such cost-benefit analyses are essential in future mission planning when uncertainty is poorly constrained, and opportunity costs are high.

This section discusses key considerations in the targeted sampling of putative microscale habitats on ocean worlds and rocky planets, as informed by applying these approaches in terrestrial settings. We further consider how we can leverage microscale, spatially resolved approaches alongside, or in place of, conventional bulk sample analyses in the search for potential biosignatures and viable life beyond Earth.

Mission science has been primarily based on near surface bulk sample analysis (e.g., Mars Science Laboratory). Future proposed missions like the Enceladus Orbilander concept (MacKenzie, Neveu et al. 2021) also rely on bulk sampling, proposing, for example, to melt and then concentrate up to 10 L of icy material to enhance the potential for microbial detection.

However, the osmotic homogenization that comes with melting icy samples may irreparably damage microbial cells living in pore spaces between ice grains saturated or near-saturated with brine (Fox-Powell and Cousins 2021). While organic compounds indicative of life, including DNA, RNA, lipids, and amino acids, will likely survive the melting process, scientists will lose the context for these potential biosignatures, making co-localization of mutually reinforcing data streams challenging. Sample return missions seek to bridge this scale gap by bringing samples to Earth-based laboratories, where researchers can perform microscale manipulations and analyses more easily.

4.1 Bulk Sampling Pros and Cons

In contrast to the microhabitat-centric focus on small (sub–cm) and spatially resolved volumes, “bulk” sampling refers to the sampling of larger areas/volumes and often deprioritizes spatial arrangements. Despite microhabitats' immense and under-appreciated value, we maintain that understanding the broader physicochemical context through bulk sampling critically clarifies whether the selective concentration of life-relevant components has occurred.

During subsurface exploration, researchers can logistically sample rock and ice in bulk more straightforwardly than through precision microsampling. For example, it does not require vehicle station-keeping or stopping within the borehole. Stopping during drilling (e.g., interrogating a specific microhabitat) can lead to the robotic vehicle or drill becoming stuck

(Glass, Fortuin et al. 2024). Therefore, bulk sampling may reduce mechanical complexity relative to targeted sampling. A greater resistance to mechanical failure or a lack of redundancy can lower both mission operational complexity and overall risk.

Bulk sampling allows scientists to continuously sample meltwater flow-through with higher temporal sampling rates in a fluid or ice-melting sampling scenario. These higher sampling rates enable filtration to gather enough material in low biomass environments to enhance the signal-to-noise ratio when the spatial arrangement is less salient.

While the burden of proof for a positive life detection result in an extraterrestrial setting may require the spatial preservation associated with microhabitat sampling, bulk sampling may best establish a true negative life detection result if, for example, scientists detected no biological molecules in the concentrate of a bulk sample comprising tens or hundreds of liters.

Bulk sampling does have its drawbacks. The physical mixing required to incorporate material from a wider volume can adversely affect biological structures or organic molecules. In ice-hosted fluid inclusions, cells in brine pockets may lyse due to changes in osmotic stress when introduced to the surrounding water.

In many ocean worlds, the lack of atmosphere means that researchers must seal boreholes fully before they can sample liquid melt. When researchers homogenize a bulk sample in rock and soil pore spaces, they can physically damage molecular structures or instigate static electrical charges that make the desorption and analysis of biomolecules especially challenging.

Furthermore, collecting material from a larger volume inherently mixes multiple layers and zones (cm– to m-scale mixing), which can dilute potential signals from regions of biological interest. Bulk sampling techniques can dilute or entirely compromise the contextual evidence required to confirm a biological result. Thus, scientists may lose confirmatory evidence even if they observe a potential positive life detection event.

4.2 Microsampling Pros and Cons

Scientists will unlikely detect life beyond Earth through a single observation “smoking gun;” rather, we anticipate multiple lines of evidence that reinforce each other. In this context, maintaining precise spatial arrangements is beneficial. For example, scientists cannot consider amino acids alone as a biosignature because many amino acids can form abiotically and have been found in meteorite samples (Pizzarello, Schrader et al. 2012, Koga and Naraoka 2017, Glavin, Burton et al. 2020, Glavin, McLain et al. 2020).

Scientists find it difficult to trust adding and subsequently visualizing a DNA-binding fluorescent dye such as DAPI as sole evidence for biological material since DAPI can bind non-specifically with mineral grains. However, when researchers see both signals co-locate—amino acids and a DNA-binding dye—they begin to build a compelling scientific biogenicity story.

The whole of multiple data streams exceeds the sum of the parts. We can make a similar case for suggestive organic-mineral associations that bulk sampling would lose. For example, a collection of iron-rich cofactor molecules (capable of biological electron transfer) and other

organics connecting two minerals of distinct redox states could suggest a metabolic redox coupling in a way that the same molecules on an inert matrix of quartz would not.

Sampling smaller volumes can also enhance signal-to-noise ratios. **Figure 4** shows a simple example, which supposes a single spherical cell of radius 0.5 μm is present in a given matrix. Assuming noise scales directly with the volume of analyzed material, the signal-to-noise ratio decreases to the cube of the analytical radius (note the logarithmic y-axis).

Many sampling approaches try to enhance signal-to-noise ratios by filtration or other concentrating techniques. This offers a promising option if researchers predominantly discard "noise" and not "signal" and if the pre-existing spatial configuration of the analyte (or the contextual surroundings) is not important. On the other hand, the value proposition of microhabitats is that 1) signal-to-noise potentially limits detecting biologically relevant materials, and 2) the spatial context of the signal is critical.

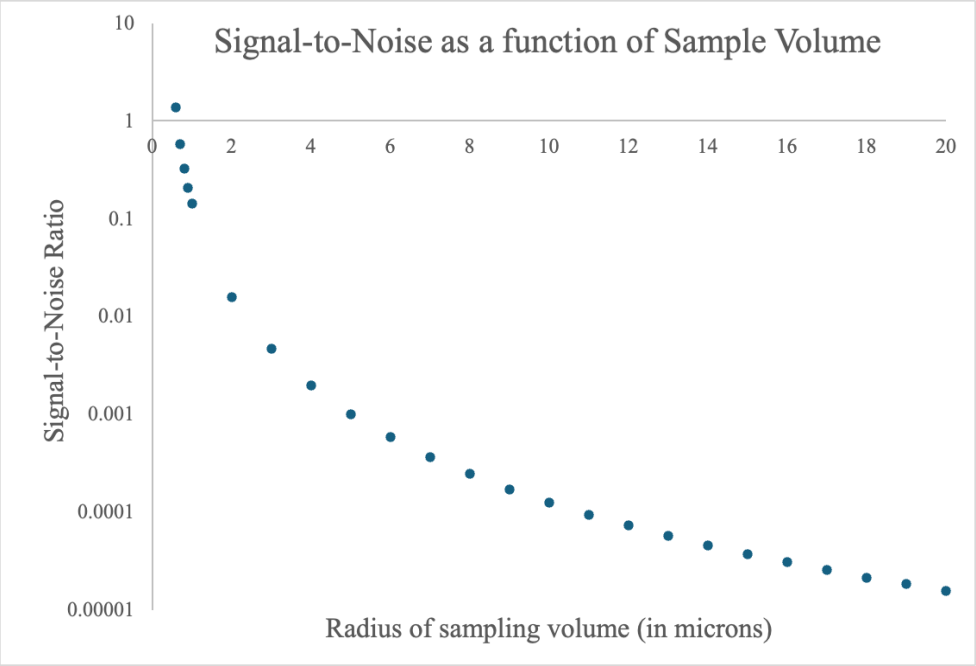

Figure 4. Plot showing signal to noise as a function of sample volume. As the volume increases, the signal-to-noise ratio drops.

On Earth, we can target and recover intact microhabitats in ice, permafrost, and rocks through detailed sampling techniques; analytical work primarily occurs not in the field but in state-of-the-art laboratories. We must develop and adapt new instrument technologies, scientific and operational workflows, and mission architectures to move toward microhabitat exploration of other planetary bodies. These scientific and engineering advances will enable us to enhance our confidence in the results of our search for life elsewhere.

5. Microhabitat Exploration and Analysis

We developed a scientific workflow for microhabitat exploration during a future planetary mission (**Figure 5**), which includes 1) detecting and initially evaluating a microhabitat region of interest, 2) deciding whether to investigate the potential biological hotspot further, and 3) extracting all or part of the microhabitat for downstream analysis. We would then bring the sample onboard a robotic platform and move it to the instrument suite, where we would first characterize it by non-destructive techniques before deciding whether further (destructive) characterization would be warranted (given limitations in sampling materials such as sample cups, derivatization agents, etc.).

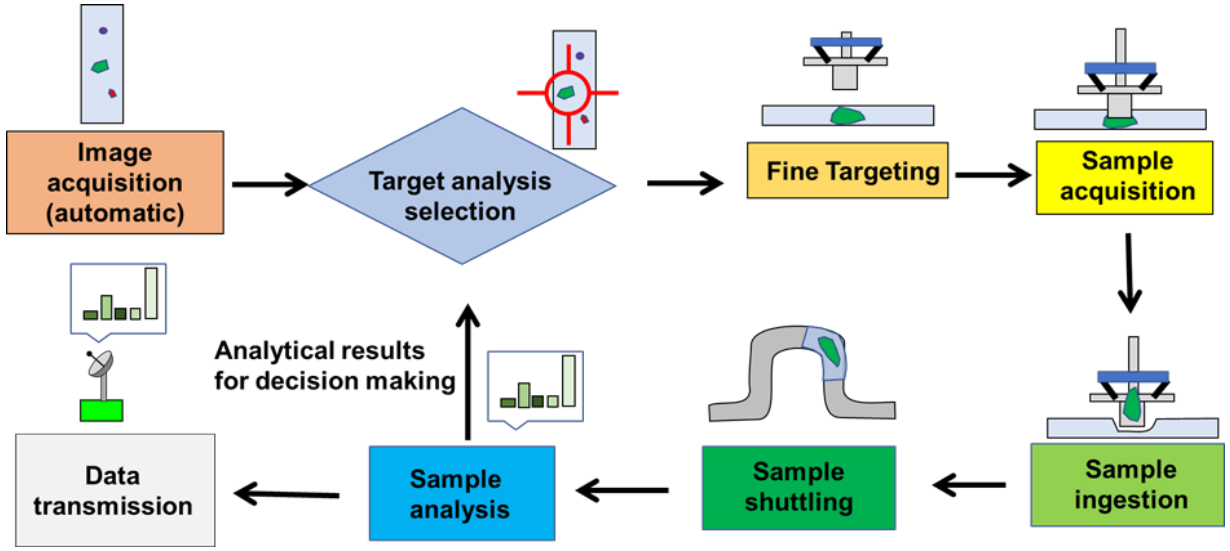

Figure 5. Flow chart for a putative astrobiology campaign from initial detection, precision targeting, sample acquisition, analysis, and transmission of those results. Following sample analysis, we could feed that information into the algorithm to determine whether or not a given signal was considered worth targeting. For example, if we determined a sample with specific spectral characteristics was uninteresting, a second target with the same characteristics may be deprioritized and not selected for acquisition and downstream analysis.

5.1 Microhabitat exploration during astrobiological exploration

Robotic architecture will determine the microhabitat detection, selection, and acquisition approach during a planetary mission. For this study, we focused on the two leading options for rocky planetary bodies containing permafrost or rock and ocean worlds: mechanical drilling and melt probe architectures.

In ice and permafrost environments, drilling technologies require near-constant motion to avoid freezing in place; however, incipient melting due to drill motion heat can provide lubrication to enable continued advancement (Glass, Fortuin et al. 2024). This factor may overcome increased friction caused by the lack of drilling fluids commonly used on Earth to enable deep drilling. Additionally, if permafrost is encountered at shallow depths, additional drill hole stabilization may provide extra time to decide about sample selection and acquisition.

Melt probes use heat to penetrate icy substrates, requiring substantial energy to turn (cryo) ices to liquid, at least temporarily, to allow the passage of a payload. This approach has several benefits, including a relatively small footprint, probe integration with a scientific payload, and fewer moving parts than a mechanical drill. Prototype melt probes have been developed and deployed in thick ice sheets on Earth, including Cryobot, Ice Diver (Winebrenner, Elam et al. 2016, Winebrenner, Burnett et al. 2024), and IceMole (Zimmerman, Bonitz et al. 2001, Dachwald, Mikucki et al. 2017) each offers a distinct heat production and fluid displacement strategy. Continued improvements in energy efficiency will be required for melt probes to be a plausible technology for mission deployment.

5.2 Identifying a putative microhabitat

Microhabitats are often characterized by elevated localized concentrations of organic molecules, redox-active molecules and minerals, and heterogeneous compositions that reflect or enable energy transfer via biological activity. Identifying the most promising volumes that could constitute a compelling microenvironment is challenging because of the uncertainty inherent in sparse initial data sets and microenvironments' small sizes and 3-D structures. Acoustic and ultrasonic approaches could be used to inform real-time analysis of potential regions of inteI rest that may harbor microhabitats using optical techniques, including Raman spectroscopy, laser-induced breakdown spectroscopy, reflectance spectroscopy, and fluorescence imaging to detect and characterize chemical, structural, and mineralogical anomalies in micro-environments (**Table 2**). Using drilling acoustic feedback in conjunction with real-time optical analyses would enable rapid identification of microenvironments of interest for downstream sampling.

Table 2. Techniques to Enable Microhabitat Detection

Technique	How is it used?	What information does it provide?
Raman mapping	A laser beam travels through meltwater and focuses on a 100 um or smaller spot on the ice wall. Meltprobe translation and vibration effectively raster laser across borehole wall to record Raman spectra continuously (20 spectra/sec). Non-destructive	2-dimensional distribution maps of ice phase, minerals, salts, organic pigments, and other potential molecular biosignatures.
LIBS mapping	A laser beam travels through meltwater and focuses on a 100 um or smaller spot on the ice wall. Meltprobe translation and vibration effectively raster laser across borehole wall to record LIBS spectra continuously (20 spectra/sec); spectra can be recorded concurrently with Raman spectra using the same hardware. Destructive.	2-dimensional distribution maps of all elements in the periodic table, organic molecules, and isotopes of interest.
UV fluorescence imaging	UV laser operating in both focused and wide-angle excites the target, and the detector captures the autofluorescence continuously. Non-destructive.	Organic compounds (aromatic amino acids, metabolic enzymes, PAHs, aromatic biomolecules), aromatized complex molecules, lignins, humic acids, fulvic acids, and mineral ions.
RGB micro-imaging	Broadband LED light travels through meltwater and focuses on the ice wall. Images can be recorded continuously (msec shutter speed) at 30 um resolution or better. Non-destructive.	Ice and rock texture, and size and shape of ice-entrained mineral grains.

Technique	How is it used?	What information does it provide?
Infrared reflectance mapping	Mid- and near-infrared LED beam travels through meltwater and focuses on the ice wall. Meltprobe translation and vibration effectively raster LED across borehole wall. Reflectance spectra can be recorded quasi-continuously (1 spectra/sec). Non-destructive	2-dimensional distribution maps of minerals, salts, organic pigments, and other potential molecular biosignatures.
Ultrasonic imaging	Focuses high-frequency sound waves into a 1 x 1 cm area on the ice wall. Meltprobe translation and vibration effectively raster waves across borehole wall. Reflected waves can be analyzed ~every second. Non-destructive.	Density and internal structure of ice, defects, cracks, and embedded materials such as rocks or sediments.

When evaluating potential instrument payloads, we must consider tradeoffs between several parameters. We must optimize analytical parameters such as sensitivity, coverage, and spatial resolution to generate optimal data. Still, we must balance these aspects against other mission directives such as time and energy use. We used characteristics of terrestrial microhabitats to determine likely fields of view required to find a microhabitat under terrestrial conditions, and we present these in Appendix 2, Figure 8: it is important to note that under nutrient-depleted conditions, the field of view could be proportionally higher. We translated this into typical scan rates for that field of view in Appendix 2, Table 7. For example, a computationally intensive, slow, on-board data processing algorithm could use precious time and energy that would otherwise enable the probe to advance further on its mission. On the other hand, a rapidly-moving probe may limit instrument integration time to a degree that limits the reliability and utility of the data.

Table 3. Order of magnitude requirements for identifying various types of features.

Feature type	FOV [mm^2]	Pixel scale [microns per pixel]	Technique Type
ROIs	1–1000	100–500	DUV fluorescence, MALDI-TOF
micropockets	1E-4–1	0.5–20	Oil-immersion microscopy, Nano-SIMS, SEM
cells	1E-4–0.1	0.1–1	Epifluorescence (DAPI, BONCAT)

Given all these considerations, we found that a continually scanning deep-UV fluorescence instrument with 100-micron context scanning resolution and 30-micron resolution provides the best balance of mission-relevant parameters for down-borehole surveys. While this option would likely miss individual cells, the greater rate of coverage—as well as the consensus consideration that microhabitats are likely to house a community of organisms- makes deep-UV fluorescence imaging for initial detection a compelling capability.

5.3 Real-time decision-making during down-core surveys

One of the biggest challenges for microhabitat detection is the need for autonomous, on-board decision-making to identify potential targets in real time. We see particular promise in the ability of optical and acoustic instruments to achieve real-time analysis and decision-making because 1) they generate data multiple times per second (which can then be processed and analyzed directly on the instruments to locate and characterize microenvironments), and 2)

they collect data in a non-destructive way that maintains all compositional information for downstream analyses. Appendix 4 details the key steps and technologies needed for the decision to extract.

Ultrasonic sensors and acoustic wave spectroscopy can locate and determine physical anomalies such as phase change and contact boundaries. Laser vibrometers and accelerometers are currently used with existing drilling technologies to predict areas where drilling faults may occur. This approach has the potential to create autonomous predictions of subsurface environmental characteristics—such as changes in hardness—to detect regions of interest that may correlate with changes in subsurface environments in permafrost (Glass, Stucky et al. 2023). However, these technologies require additional development for ocean world applications as it may be more difficult to detect microscale features with increasing depth in the ice shell.

5.4 Targeting the Spot

Once we decide to extract a putative microhabitat based on *in situ* surveys, the mechanical process of physically isolating and transporting the volume of interest will occur. A technical challenge will be passing along the targeting information, whether cartesian x, y coordinates or polar z, theta coordinates to a static reference frame for precision placement. Due to the small size of the target, precision lineup is critical and technically challenging. A pass-through of information from the initial detection to the mechanical targeting system is key.

5.5 Microhabitat Extraction Methods

We highlight several sampling systems (some integrated with analytical payloads) at different development levels, ranging from concepts to flight systems (**Table 4**). There are also sampling systems developed for Earth applications that range from human-in-the-loop to full autonomy. Some of these systems have the potential to be scaled to address microsampling in planetary environments.

Common challenges for these and other drilling and coring platforms include 1) cross-contamination between different drill bits, 2) mechanical wear of the drill bit (including the introduction of microscopic fragments to the environment), 3) the acquisition of intact, consolidated cores, 4) the maintenance of fully solid, unmelted volumes when drilling in ice and permafrost, and 5) contamination of biological and chemical components from higher in the drilled section through “smearing.”

Integrating a separate section with isolated anchoring and station-keeping capabilities would allow sampling without placing stringent mechanical requirements on the primary spacecraft to perform these functions. Small corers, equipped with rotary hammer drill bits or drive tubes, small scoops, independent actuation, and retracting mechanisms, meet this challenge and should be prioritized in future mission development.

We call for the prioritization of sample collection approaches that are mechanically simple, adaptable to a range of distinct material properties, and fast. One common source of complication and sample handling errors is the transfer from a collection vessel (e.g., a drill

tube) to the analytical vessel (e.g., an onboard instrument platform). Developing integrated sampling and analysis architectures whereby the analyses are conducted directly on/from the sampling tube would eliminate the need for sample transfers and minimize sample disintegration and loss. Below, we present some of these planetary exploration concepts that could be implemented for microhabitat sampling and sample transfer:

Table 4. List of sampling instruments relevant to microhabitats.

Instrument	Description	Sample Type (Amount)	Technology Readiness Level
The Regolith and Ice Drill for Exploration of New Terrains (TRIDENT)	TRIDENT delivers volatile-rich samples up to 1 m depth to the lunar surface. Mass spectrometry and infrared spectroscopy would then analyze the material to determine volatile composition and mineralogy.	Powder from subsurface regolith; (~1 g or 1 cm^3 of material collected)	9
Precision Subsampling System (PSS)	The PSS selectively acquires samples (dry cuttings) with mm scale resolution from a host rock core. Sampled cuttings are then subjected to chemical and mineralogical analyses.	Cuttings from rocks; (100 ug to 10 mg is collected)	4-5
Micro In-Situ Tomography (MIST)	MIST conducts in situ analysis of planetary samples, including ice and rock. A core is collected in an X-ray transparent tube, and X-ray attenuation images are acquired; these images will be processed to make a 3D digital volume of the core, allowing the characterization of features ≥ 20 μm in size.	Intact cores of ice and rock (2.5 cm in diameter)	3-4
Rotary Percussive Coring Drill (RoPeC)	The RoPeC drill can use different drill bits for different applications, including a coring bit to capture core samples, a PreView bit to allow the core to be inspected in situ, a Powder Bit to allow for capture of regolith and rock cuttings, and a Rock Abrasion and Brushing Bit to brush and grind rocks.	Regolith, rock cuttings, or intact rock core, (1 cm in diameter)	6
NanoDrill	The Nano Drill is a portable, small-scale coring drill that can be integrated with other systems, such as drones and rovers.	Rock core, 1 cm in diameter, 2-3 cm long) (1.6–2.4 cm^3)	4-5
Kinetic Rotary Acquisition Kit for the Excavation of Nautical Substrate (KRAKENS)	KRAKENS is integrated with a combination Laser Raman Spectroscopy / Laser Induced Native Fluorescence instrument to conduct initial chemical characterization and sampling in an underwater setting.	Rock core, 1.9 cm in diameter, 11.4 cm long	6

Common challenges for these and other drilling and coring platforms include 1) prevention of cross-contamination between different drill bits, 2) mechanical wear of the drill bit (including the introduction of microscopic fragments to the environment), 3) the acquisition of intact, consolidated cores, 4) the maintenance of fully solid, unmelted volumes when drilling in ice and permafrost, and 5) prevention of sample contamination of biological and chemical components from higher in the drilled section through “smearing.”

For the remote drill system, which returns a sample to a surface element for detailed analysis, in addition to sampling system constraints by the descending probe, the primary spacecraft (to

which the sample is returned for more thorough analysis) is also subject to various considerations. Integrating a separate section in the sampling system with isolated anchoring and station-keeping capabilities would allow sampling without placing stringent mechanical requirements on the primary spacecraft to perform these functions. Small corers, equipped with rotary hammer drill bits or drive tubes, small scoops, independent actuation, and retracting mechanisms, meet this challenge and should be prioritized in future mission development.

In the context of an interplanetary mission, which will be drastically constrained in terms of time, space, and repair contingencies, we call for the prioritization of sample collection approaches that are mechanically simple, adaptable to a range of distinct material properties, and fast. One common source of complication and sample handling errors is the transfer from a collection vessel (e.g., a drill tube) to an analytical vessel (e.g., an onboard instrument platform). Developing integrated sampling and analysis architectures whereby the analyses are conducted directly on/from the sampling tube would eliminate the need for (at least some) sample transfers and minimize sample disintegration and loss. The MIST instrument highlighted in Table 4 is one example: X-ray transparent tubes are used for collection, enabling analysis by X-ray tomography without sample transfer.

5.6 Key Developmental Considerations for Microhabitat Extraction

The most significant challenges of extraction are the preservation of the microhabitat and the speed and accuracy of the extraction step. Inherent to any extractor design is the breaking apart of the surrounding substrate (ice and/or rock), which poses risks of damage to the volume of interest. Mechanical destruction may lead to habitat exposure to a different thermal, pressure, or saline environment, causing unwanted chemical stability or microbial metabolism modifications. This issue has been observed during drilling in permafrost, where drill string heating can melt the surrounding ice, leading to limited sample retrieval.

Depending on the host vehicle architecture, the probe may have a limited ability to stop or slow its rate of descent. For example, an RTG-powered probe could overheat rapidly should its descent be paused, even for a short time. In this context, the extraction system would need to run through operations without significantly affecting the probe descent speed, which is on the order of meters per hour (or millimeters per second). Targeting a microenvironment while in motion is another technical challenge, as the process must be fully autonomous, and most microhabitat targets are smaller than current technology developments typically extract.

An architecture with an inch-worming approach, such as what was used in the Deep Drill design on the Greenland microhabitat study (Rafeek, Gorevan et al. 2001, Malaska, Bhartia et al. 2020) would allow for better control of the descent speed and could pause the cryobot for a short time. Using a different power source, such as the Kilopower reactor, which uses fission, may also allow for the cryobot to pause in place during sample acquisition or other sensitive events. An alternative approach for dealing with cryobot motion is to have a vertical degree of freedom for the extractor, which could be a follower system that stays behind in the melt pocket to conduct mechanical and scientific operations. These challenges of station keeping

and microhabitat sample extraction in a way that does not negatively impact drill or probe descent have been understudied and remain non-trivial. This area warrants focused attention to enable a future mission to target microhabitats for life detection.

Table 5. Excised volume characteristics for extracted features.

Feature Type	Excision diameter range [microns]	Excision cell counts range [cells]	Excision volumes range [microliters]	Excision Effective cell concentration range [cells per cm^3]
ROIs	500-10,000	100-20,000	2-1000	1E4-5E5
micropockets	20-300	0.1-20	1E-3-1	5E2-5E6
cells	2-30	1	1E-5-1E-2	1E5-5E7

6. Conclusion and Key Findings

The identification, sampling, and analysis of microhabitats carry excellent potential for future astrobiological investigations. However, to fully realize this potential, the astrobiology, robotics, microbiology, and planetary science communities must work together to address key technology, science, and funding gaps. In particular, we recommend the following areas of priority and focus:

To further develop the intellectual grounding and community support for microhabitat study, an effort should be made to configure the “Standards of Life” to microhabitat and microscale analyses.

We recommend adapting current analytical instrumentation and techniques for small sample volumes in the microliter to nanoliter range for detailed astrobiological analysis of microhabitats. We recommend investments to adjust the compendium of “life” tests (i.e., chirality, morphology, isotopes) recommended by the astrobiology community to use 1-2 microliters to nanoliters of total sample volume.

For initial detecting ROIs and microhabitats, we recommend investment in developing and ruggedizing a DUV fluorescence/optical imaging system, including epifluorescence-staining techniques for in situ biosignature investigation.

We recommend the development of information-transfer, automated decision-making, and robotics technologies to detect, prioritize autonomously, and target microhabitats for extraction given an initial instrument image. Necessary technologies will push the limits of small-scale, precision engineering.

We also recommend carrying out further in situ exploration of ocean-world-like terrestrial environments: ocean ice, ice sheets, deep-sea sediments, ocean-ice interface, rock-air interface, in situ deep ice (drilling), deep rock (drilling) to not only test and assess the performance of instrumentation and techniques.

Given the interdisciplinary nature of astrobiological microhabitat studies, we recommend specific microhabitat-focused funding streams, which may encompass priorities from multiple existing programs such as PICASSO/MATISSE, Exobiology, SBIR, and PSTAR.

Appendix 1. Scale of microhabitats: Characteristics of different scales of microfeatures.

From the literature, we extracted and mapped features found in images of microenvironments from terrestrial samples analogous to Ocean world habitats (**Table 6**). We found natural breaks in scale. We identified these as larger Regions of Interest (ROI), micropockets (semi-enclosed environments containing multiple cells), and the microbial cell at the smallest scale. The cell represents the smallest living environment since it cannot be subdivided further.

Table 6. Examined datasets, instrument techniques, and references.

Entry ID	Type Feature	Sample Type	Technique	Reference
Entry 1	ROI	snowfall firn	Deep UV fluorescence mapping	Malaska et al., in prep1, 9.129 m firn
Entry 2	ROI	snowfall firn	Deep UV fluorescence mapping	Malaska et al., in prep1, 20 m firn
Entry 3	ROI	snowfall glacial ice	Deep UV fluorescence mapping	Malaska et al., in prep1, 84 m glacial
Entry 4	ROI	snowfall glacial ice	Deep UV fluorescence mapping	Malaska et al. (2020), 93.8 m glacial
Entry 5	ROI	snowfall glacial ice	Deep UV fluorescence mapping	Malaska et al., in prep1, 93.8 m glacial, different borehole azimuth
Entry 6	ROI	snowfall glacial ice	Deep UV fluorescence mapping	Malaska et al., in prep1, 101.668 m glacial
Entry 7	ROI	snowfall glacial ice	Deep UV fluorescence mapping	Malaska et al., in prep1, 106.7 m glacial
Entry 8	ROI	snowfall firn	Deep UV fluorescence mapping	(Rohde 2010), Fig 32a
Entry 9	ROI	snowfall firn	Deep UV fluorescence mapping	(Rohde 2010), Fig 32b
Entry 10	ROI	snowfall glacial ice	Deep UV fluorescence mapping	(Rohde 2010), Fig 32c
Entry 11	ROI	snowfall glacial ice	Deep UV fluorescence mapping	(Rohde 2010), Fig 32d
Entry 12	ROI	snowfall glacial ice	Deep UV fluorescence mapping	(Rohde 2010), Fig 32e
Entry 13	ROI	snowfall glacial ice	Deep UV fluorescence mapping	(Rohde 2010), Fig 32f
Entry 14	micropocket	sea ice	oil-immersion microscopy	(Junge, Eicken et al. 2004), Fig 1a
Entry 15	cell	sea ice	epifluorescence (DAPI)	(Junge, Eicken et al. 2004), Fig 1a
Entry 16	micropocket	sea ice	oil-immersion microscopy	(Junge, Eicken et al. 2004), Fig 1b
Entry 17	cell	sea ice	epifluorescence (DAPI)	(Junge, Eicken et al. 2004), Fig 1b
Entry 18	micropocket	sea ice	oil-immersion microscopy	(Junge, Krembs et al. 2001), Fig 6
Entry 19	cell	sea ice	epifluorescence (DAPI)	(Junge, Krembs et al. 2001), Fig 6
Entry 20	cell no diatoms	sea ice	epifluorescence (DAPI)	(Junge, Krembs et al. 2001), Fig 6

Entry ID	Type Feature	Sample Type	Technique	Reference
Entry 21	ROI	lake ice	532 nm Laser Induced Fluorescence (LIF)	(Sattler, Storrie-Lombardi et al. 2010), Fig. 7 (Spot 186)
Entry 22	ROI	lake ice	532 nm Laser Induced Fluorescence (LIF)	(Sattler, Storrie-Lombardi et al. 2010), Fig 7 (Spot 188)
Entry 23	ROI	lake ice	532 nm Laser Induced Fluorescence (LIF)	(Sattler, Storrie-Lombardi et al. 2010), Fig 7 (Spot 189)
Entry 24	ROI	lake ice	532 nm Laser Induced Fluorescence (LIF)	(Sattler, Storrie-Lombardi et al. 2010), Fig 7 (Spot 191)
Entry 25	ROI	lake ice	532 nm Laser Induced Fluorescence (LIF)	(Sattler, Storrie-Lombardi et al. 2010), Fig 7 (Spot 192)
Entry 26	ROI	refrozen supraglacial lake	Deep UV fluorescence mapping	Malaska et al., in prep2, 0.32-0.35 m deep
Entry 27	ROI	refrozen supraglacial lake	Deep UV fluorescence mapping	Malaska et al., in prep2, 0.39-0.46 m deep
Entry 28	ROI	refrozen supraglacial lake	Deep UV fluorescence mapping	Malaska et al., in prep2, 0.39-0.46 m deep, puck
Entry 29	ROI	refrozen supraglacial lake	Deep UV fluorescence mapping	Malaska et al., in prep2, 0.39-0.46 m deep, high-resolution puck subsection
Entry 30	ROI	bottom lake sediments	Mass spectral imaging (MSI)	(Obreht, Wörmer et al. 2020), Fig 2
Entry 31	micropocket	microbial mat	nano-SIMS 32S abundance	(Fike, Gammon et al. 2008), Fig 3b
Entry 32	micropocket	microbial mat	nano-SIMS 32S abundance	(Fike, Gammon et al. 2008), Fig 3d
Entry 33	micropocket	fumarole	eSEM	(Marlow, Colocci et al. 2020), Fig 1i
Entry 34	cell	fumarole	epifluorescence (BONCAT)	(Marlow, Colocci et al. 2020), Fig 1i
Entry 35	micropocket	fumarole	eSEM	(Marlow, Colocci et al. 2020), Fig 1ii
Entry 36	cell	fumarole	epifluorescence (BONCAT)	(Marlow, Colocci et al. 2020), Fig 1ii
Entry 37	micropocket	fumarole	eSEM	(Marlow, Colocci et al. 2020), Fig 1iii_above
Entry 38	cell	fumarole	epifluorescence (BONCAT)	(Marlow, Colocci et al. 2020), Fig 1iii_above
Entry 39	micropocket	fumarole	eSEM	(Marlow, Colocci et al. 2020), Fig 1iii_below
Entry 40	cell	fumarole	epifluorescence (BONCAT)	(Marlow, Colocci et al. 2020), Fig 1iii_below
Entry 41	ROI	evaporite	Deep UV fluorescence mapping	Malaska et al., in preparation[3], borate crystal

We present the average size distribution of features found in different images from terrestrial analog environments in **Figure 6**. The entries have been re-sorted by feature type and based on approximate location along a theoretical transect from the top surface to the deep ocean

bottom of an example Ocean World. Several features in the supraglacial melt pond ice (Entries 26 to 29) may be sections of microbial mat that became free-floating before being frozen as the pond solidified; since it was embedded in the ice, we counted it as an ROI.

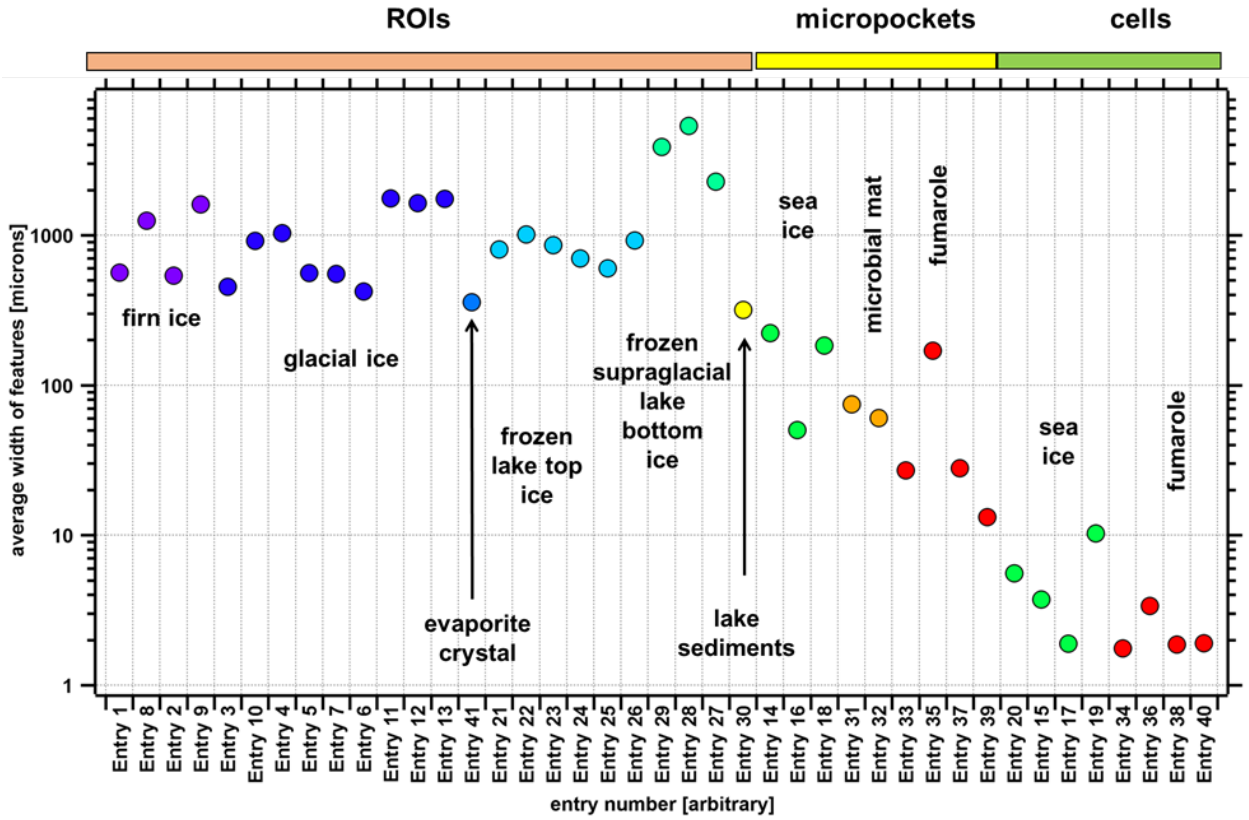

Figure 6. The average size distribution of features found in different images from terrestrial analog environments to the average width of terrestrial samples analogous to Ocean world habitats. Data from analysis of sources in Table 6.

The x-axis presents entries correlated to feature types from larger ROIs on the left to micropockets, to cells on the right (**Table 6**). Colored markers correspond roughly to the depositional environments from the top surface in cold tones to deeper subsurface environments in warm tones. For firn ice and glacial ice (dark purple and blue), increasing the entry number from left to right corresponds to a rough increase in depth on a meter to 10s of meters scale. The Y-axis shows the average maximum length of the features in that mapped entry.

Due to the resolution requirements, at least two pixels will be necessary to confirm a feature is not a “hot pixel” and be able to provide corroborating spectral data that would give confidence that a target is real. Given the dimensions in **Figure 6**, we show the minimum pixel scale for an imaging instrument to identify and provide precise targeting information for an ROI, microhabitat, or microbial cell in **Figure 7.** The size of the target feature will drive instrument pixel scale requirements. The key difference is if simple localization (one pixel) or detailed identification (multiple pixels) is required. Localization will be required for target acquisition, but identification may be needed to determine if the target is of sufficient interest. Localization

might be possible near the pixel scale of a given feature. Still, for identification that the feature is of interest, pixels scales smaller than the target feature are required to reveal identifying morphologies. For example, for bacterial cells on the order of 1 micron, a resolution of at least 0.5 micron per pixel would be required for spatial location. Still, ideally, a 0.1 micron per pixel image scale would enable bacterial cell identification. Larger cells, such as diatoms, can be detected with a 1-micron-per-pixel scale. However, higher-resolution imaging will allow the detection of diagnostic morphologic features such as puncta, rapheae, and girdle bands. Micropockets can be detected with imaging from the 1 to 10 micron scale. For ROIs, imaging at the 100 microns per pixel to 400 microns per pixel scale is sufficient.

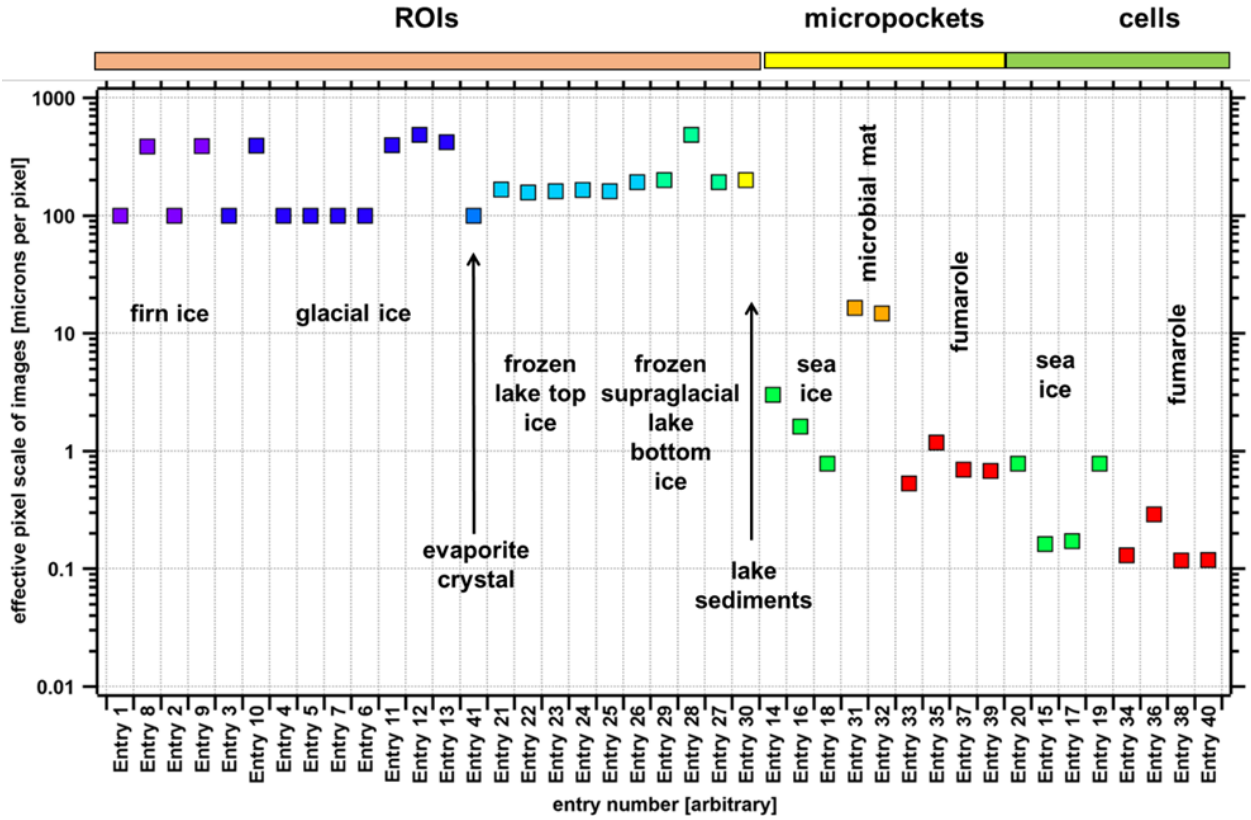

Figure 7. A pixel scale is required to detect various features. Data from analysis of sources in Table 6.

A pixel scale of 100 microns per pixel for ROIs is enough for feature detection. Due to their smaller dimensions (**Figure 6**), a finer pixel scale is required for micropockets.

Appendix 2. Scan rates to detect features

From the analysis of microhabitat images in Appendix 1, Table 6, we determined the largest circular area in each image that could be drawn, encompassing an area with no evident targets (ROI, micropockets, or cells, as appropriate). This represented the maximal circular area that could be scanned in that image, which would not have a target object detected. Thus, any examined circular area larger than this would have at least one target object present. This approach represents a practical value based on actual observations. For practical application,

any instrument searching a given image must have a field of view larger than the void region to guarantee the detection of a target.

The results are plotted in **Figure 8.** The type of target feature determines the required field of view. For example, to guarantee the detection of an ROI, the circular field of view needs to be in an order of 1 to 1000 mm^2 (roughly a square inch). For micropockets, a circular field of view must be from 0.01 mm^2 to 1 mm^2 in ice and from 0.0002 mm^2 in hydrothermal rock to guarantee detection. For the much smaller cells, FOVs of 0.0001 mm^2 to 1 mm^2 at pixel scales less than 1 micron per pixel are required to detect bacterial cells.

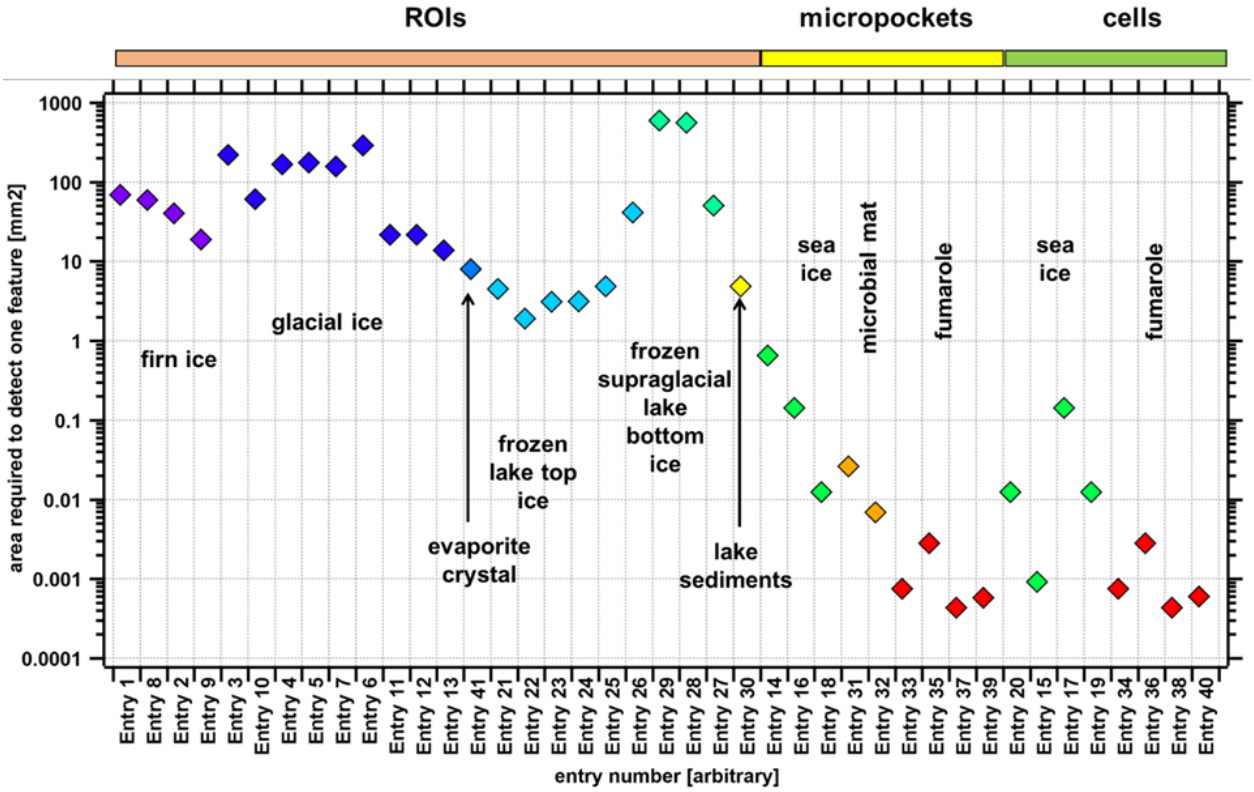

Figure 8. Minimum fields of view are required to detect a single feature. This is based on the largest circle in the analyzed scene for each entry that did not contain a feature. At least one feature would be detected for any field larger than this area. Data from analysis of sources in Table 6.

Given the required field of view and the various instrument scan times to complete a raster of a given size, we prepared an estimated scan time to scan the necessary Field of View (FOV) to guarantee feature detection. This is presented in **Table 7**.

Table 7. Scan times required to detect one feature

Instrument type	DUV fluorescencse, MALDI TOF	Oil-immersion microscopy, Nano-SIMS, SEM	Epoifluorscence (DAPI, BONCAT), SEM
Minimal FOV (field of view)	1.9-598 mm^2	400–700,000 $microns^2$	400–140,000 $microns^2$
Estimated scan time	69-167 sec	210–1021 sec	53–1015 sec
(Basis of estimate)	100-micron pixels at 100 Hz for DUV data	500 square microns in 180 sec for SEM data	500 square microns in 180 sec for SEM data

Appendix 3. DUV molecules

Detection of extant microbial life elsewhere in the solar system will almost certainly require microscopic imaging techniques, as purely chemical techniques—which have been referred to as detection of "substances" (Chan and et al. 2019)—do not distinguish between extant life and proto-life or abiotic complex chemistry (Cleaves 2012). Microscopy adds the detection of "objects" to "substances," which can yield key morphological biosignatures such as cells and microfossils (Chan and et al. 2019). The design of a microscope for life detection is challenging, involving trade-offs between spatial resolution, volume of view, speed of throughput, and choice of biosignature to target.

Label-free techniques targeting bacterial autofluorescence are particularly interesting because they minimize sample handling and alteration, and because dyes can degrade during storage and pose planetary protection concerns. However, autofluorescence produces relatively weak and nonspecific signals. Quantum yields of native fluorophores are almost always much lower than those of dyes (usually < 1%), or the molecules are present at very low concentrations, making spectral separation from the background a critical capability. One exception to this general rule is chlorophyll, which shows emission more intense than most dyes; it provides valuable autofluorescence signatures even in endolithic microhabitats (Roldan, Ascaso et al. 2014).

All fluorescence analyses involve the introduction of light of a certain wavelength to "excite" electrons to a higher energy level (a process known as excitation), as well as the production of light at a longer wavelength (emission). Excitation may be in the deep UV, near UV, blue, or green. Each wavelength range has advantages and disadvantages: deep UV, for example, requires specialized optics, while near UV excites more background from minerals or surfaces. Emission signals can be distinguished based on color (Dartnell, Storrie-Lombardi et al. 2010), Stokes shift (Bittel and et al. 2018), or fluorescence lifetime (Berezin and Achilefu 2010, Datta, Gillette et al. 2021), which may be measured quantitatively or used as a gate to exclude unwanted signals (Shkolyar, Eshelman et al. 2018, Yang and Chen 2020) **Figure 9** shows absorbance and emission spectra for key molecules involved in microbial autofluorescence. Excitation/emission wavelengths and quantum yields are in Table 8. Many datasets do not provide absorbance values below 300-350 nm, so it is important to verify values in the UV when these are of interest.)

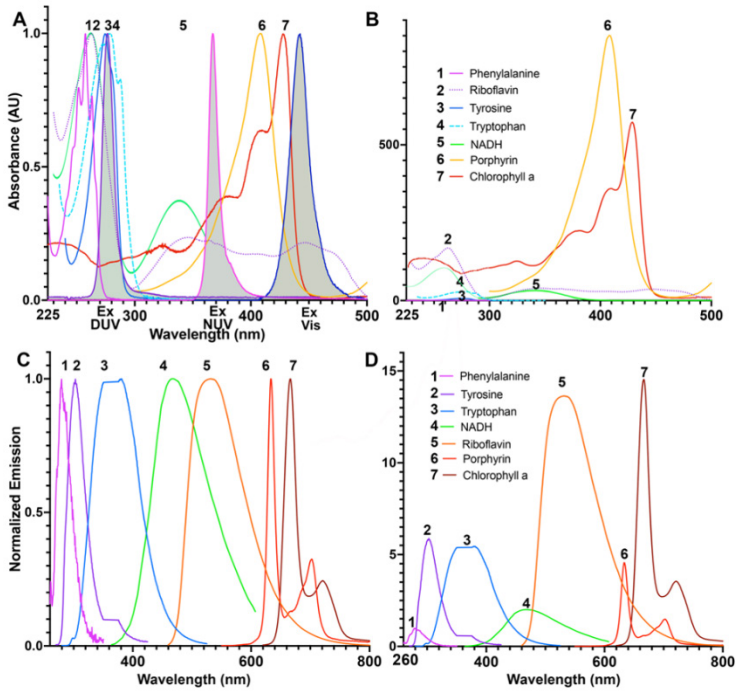

Figure 9. Molecules responsible for microbial autofluorescence. (**A**) Absorbance spectra of key autofluorescent biological molecules. The gray-shaded curves indicate excitation spectra in Deep UV, Near UV, and Visible excitation. NADH was normalized to its peak at 250 nm, although the peak at 340 nm was used for imaging. (**B**) Absorbance spectra are scaled by the magnitude of the extinction coefficient at the wavelength usually used for excitation. (**C**) Normalized emission spectra of the selected molecules. (**D**) Emission spectra scaled by quantum yield when excited at typical wavelengths (**Table** 8) (Spectra and quantum yields as reported in PhotoChemCad https://www.photochemcad.com/).

While autofluorescence is a useful, nondestructive, noncontact technique, it is not necessarily diagnostic of life. Emission spectra represent electronic transitions that are general to broad classes of molecules. For example, the tryptophan-like peak corresponds to molecules with at least one aromatic ring, including amino acids, indoles, polycyclic aromatic hydrocarbons (PAHs), and other biogenic and abiogenic compounds. Emission in the blue to green range results from molecules with two or more aromatic rings and quinones, flavonoids, and PAHs (Coble, Spencer et al. 2014, Carstea, Popa et al. 2020). The value of cellular autofluorescence lies in its combination with microscopy, where sufficient contrast with the surrounding substrate can reveal objects with cell-like morphology and possibly subcellular structures, which, especially when present in a repeating pattern, can be highly suggestive of life forms. Thus, while autofluorescence is not a direct indicator of life, it can be used to indicate and triage samples for further examination.

Table 8. Fluorescence quantum yields and absorption coefficients of various molecules responsible for cellular autofluorescence.

Molecule	Excitation used for QY measurement (nm)	Emission peak (nm)	Quantum yield	Molar extinction coefficient (M^{-1} cm^{-1})
[1]Phenylalanine	240	280	.022	195
[1]Tyrosine	260	304	.13	1405
[1]Tryptophan	270	355	.12	5579
[1]Riboflavin (in ethanol)	450	530	.3	33000
[2]NADH	340	460	Variable	
[1]Protoporphyrin IX (in chloroform)	407	633	.06	171000

Table 8: Photophysical parameters of biomolecules reported in spectral databases: [1]PhotochemCAD; [2] (Ma, Digman et al. 2016)

Appendix 4. Determining Whether to Extract a Microhabitat Sample

The combination of constrained onboard processing power, minimal outside communication, and finite consumables (e.g., reagents or sample tubes) limits the number of sampling opportunities. In the case of ice penetration (for example, a melt probe descending through the icy crust of an Ocean World), there is an added complication: the probe must execute a continuous descent to avoid the "start-up" thermal and energy costs associated with remelting the ice front. This means a melt probe will have limited time to decide whether to sample an identified microhabitat.

Continuous measurements of the macroenvironment—including temperature gradients, changes in pH, and compositional/textural patterns in the surrounding matrix—are key measurements that can guide the search for regions of interest that may be targeted for additional analysis. In conjunction with acoustic and optical data, these relatively large spatial scale measurements will feed into a Bayesian decision framework to assess the sensor inputs and decide when to initiate the sampling process. This framework will fuse the observations made from the onboard instruments, weigh the different observations based on ground-truthed models linking observables with biogenic potential, and decide whether an area is likely to contain microhabitats. If the decision is affirmative, the sample acquisition process will be triggered (Error! Reference source not found.).

Developing this decision framework presents significant challenges. The expected state of the environment will not be fully known in advance, creating uncertainties about the expected distribution of sample data and noise in the measurements. Communication, energy, and time constraints eliminate human-in-the-loop decision-making, such as those used in recent near-surface sampling protocols on Mars. Distant and deep subsurface missions will have limited communication, thus forcing the exploration system to be fully autonomous for its sampling and decision-making progress. This is especially challenging given the uncertainty and limited ground truth data from environments containing the microhabitats.

Several theoretical frameworks exist for dealing with such uncertainty. While this is not an exhaustive survey, several promising approaches exist. One is the partially observable Markov

decision processes (POMDPs), which treat the existence of microhabitats as the state of the system that it may collect noisy observations on in an attempt to determine its actual state while considering constraints on energy, communications, and consumables (Burks, Ray et al. 2023). A key consideration is the balance between near- and long-term rewards, such as whether to continue to sample a promising area against the possibility that an even better location may appear.

Another such approach is reinforcement learning (RL), where the probe learns online from the results of its actions to sample the environment. RL has seen great interest from the machine learning community in recent years due to its ability to learn complex environments and relationships between variables in the environment (Jayaraman and Grauman 2018, Colander, Bekski et al. 2021, Brumwell, Kitchen et al. 2023, Ravier, Garagić et al. 2023).

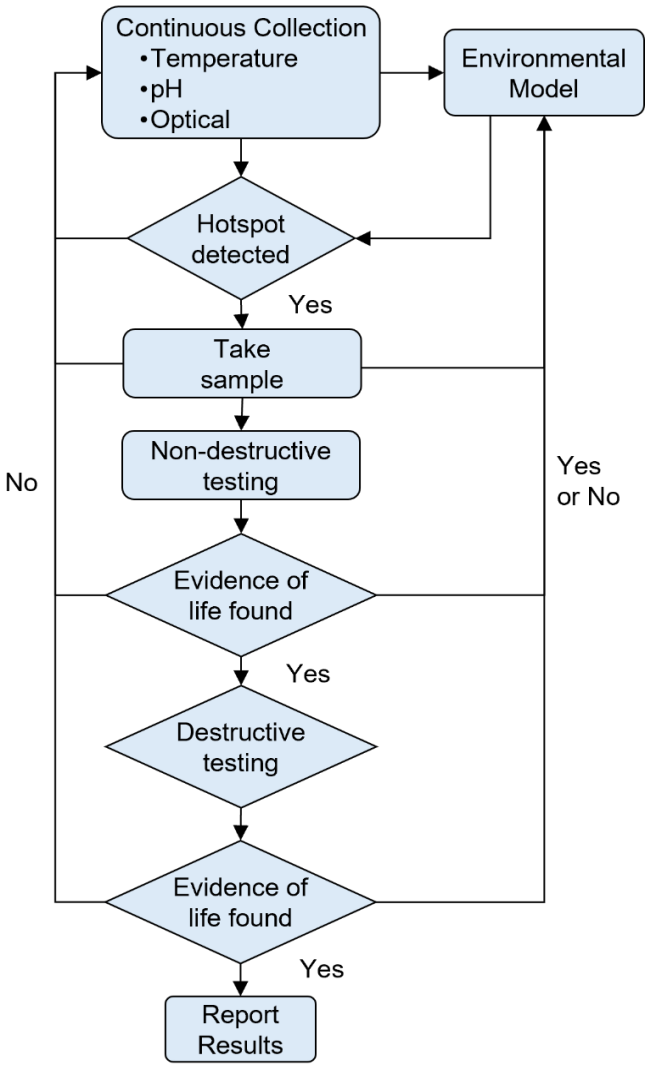

Figure 10. A flow chart is used for information flow in the decision process for sample acquisition. This also incorporates the results of previous samples as part of the decision-making process. If similar samples are not deemed interesting, then this sample will be deprioritized. If this is dissimilar to previous samples, it will be considered novel and prioritized for analysis.

However, a continuously moving probe presents significant challenges to RL approaches. For example, as the probe descends, its environment will change and evolve, limiting the utility of the information gained from sampling performed early in the mission. Constraints on consumables and time-on-target limit how many attempts the probe can make to learn its environment, further constraining its ability to create effective policies for its mission. Finally, the limited computing resources on board the probe and potentially available at the surface of the deployment create significant hurdles. Recent advances in the robotics and machine learning communities may solve some of these problems, but considerable research is needed for this application.

Anomaly detection is an area that has seen major advances in recent years that may be relevant to microhabitat applications (Li and et al. 2022, Huang and et al. 2023, Shi, Mao et al. 2023).

Anomaly detection seeks to find statistical outliers from an underlying distribution without prior knowledge of the expected state of the system. Modern machine learning (ML) approaches have significantly improved on simpler statistical tests, enabling modern anomaly detection algorithms to process non-linear and high-dimensional data distributions effectively. These systems can also learn online, enabling the probe to adapt to its environment after deployment.

All these approaches will benefit from extensive testing in surrogate and simulated environments before deployment. Developing the decision framework in these environments allows engineers and scientists to consider a wide variety of possible scenarios and to leverage much larger computational resources to create models and policies for processing data. The final probe may contain an ensemble of models, select the best-fit model once deployed, and adapt it based on its in-situ measurements.

While near-surface sampling on Mars uses human-in-the-loop decision-making protocols, current efforts are underway to improve autonomous drilling activities for future Mars missions like Mars Life Explorer ((NASA) 2021)or the Icebreaker Discovery Mission Concept (Glass, Heldmann et al. 2023). Due to their distance and lower communication rates, Deep Ocean World drilling expeditions will likely never be capable of making decisions in a human-in-the-loop manner. Therefore, it may be possible to test and refine these decision protocols in a lower-risk environment such as Mars before proceeding to full autonomy in an ocean world environment where communications delays preclude human-in-the-loop decision-making. Mars drilling missions can be a testbed for more challenging Ocean World applications.

Appendix 5. Proposed Microhabitat Extraction Developmental Pathway

Our evaluation of existing sampling systems for microscale environments revealed a substantial and concerning gap between operational and scientific needs and existing technology. Without extended research and development programs conducted alongside scientific interrogation of the microhabitat concept, chances of successful life detection endeavors will be low. We propose a pathway toward effective microhabitat interrogation, described here from an engineering perspective.

Potential sampling systems for mission use would first be designed as a proof of concept tool and tested from a stable platform. The collection and retention of an ice, permafrost, regolith, or rock sample at the sub-cm scale in a dry or wet environment must be demonstrated. Subsequent generations of the system would be multi-use: for example, they could be purged and cleaned, they could replace the sample collection tool, or they could extract more than one sample for analysis. These future systems would also be able to collect samples from a moving platform without the need for the drive vehicle to stop. Lastly, once these systems have been proven individually, sampling and analytical functions must be integrated with control software to demonstrate an end-to-end sample detection, collection, and transfer process. These efforts will, therefore, require both instrument development programs and future field and laboratory demonstrations before a microhabitat detection and extraction system is ready for flight.

We propose a common testbed plan to fulfill this challenge by evaluating whether the system can (1) sample the target material, (2) accurately target the microhabitat of interest, and (3) maintain the sample integrity, keeping the microhabitat intact for the science instruments.

The sampling system must be able to separate the microhabitat from its surrounding environment. Current techniques include physical isolation and manipulation (e.g., breaking apart the target and recovering it with a manipulator) or suctioning methods that use negative air pressure to move volumes of interest. The testbed analog needed to evaluate this capability must consider the analog material's temperature, salinity, structure, and pressure environment. Existing testbeds, such as the high-pressure chambers at SWRI or JPL's CITADEL chamber, are good examples of relevant chambers that could be used for future sampling system development.

Accurately targeting the microhabitat within the sampled material involves an autonomous targeting system and a simulated target. A testbed would need a way to simulate a microscale target (e.g., through fluorescent or other compositionally distinct microscale beads) as well as the motion of the target volume relative to the sampler.

The most challenging and underdeveloped part of the microhabitat workflow is the maintenance of sample integrity. A testbed for this capability must include a microenvironment whose "intactness" can be characterized before and after the sampling event. The microenvironment could be a biological microhabitat or some other abiotic simulant, and potential indicators of structural integrity could include electrically conductive nanowires/cells, spatially separated dyes, or pre and post-X-ray tomography scans.

We envision a tiered approach for testbeds as the degree of mission realism and system complexity increase. Initially, test beds can be simple, small-scale ice or rock blocks kept stationary. Such setups would involve a pre-determined, pre-seeded microhabitat at a known location within a fixed simulant. The sampling system would then move through the volume and sample as appropriate. At the next level of complexity, we anticipate tests of the sampling system in motion. The size of the associated testbeds should be constrained to 2-3 times the size of the test vehicle to avoid wall effects in which physical properties near edge zones may vary from the bulk simulant. In this case, testing may involve a pre-drilled hole with the sampling system moved within it at a predefined speed. This process simulates the architecture of a constantly descending cryobot that cannot pause for sampling operations. (A situation in which both components of the process—sampler and target—are in motion represents a unique challenge with no current solution. The degree to which this possibility is likely to be encountered remains uncertain but is not currently a focus of mission projections.)

The last physical testbed would be suited for a system-level test, in which the microsampler is integrated into a vehicle, such as a melt probe. The testbed must be large enough for vehicle motion and full system operation. This arrangement can accommodate short depths (on the order of a few meters) in the lab, but field analog sites are currently better suited for this level of testing. Field-based testing is also useful for anomaly detection, as the subsurface in the field often represents a true unknown environment that can test inherent assumptions that may be

built into future testbed set-ups. (Glass, Fortuin et al. 2024) has a good discussion of this. Finally, we note that computer-simulated environments can be important testbeds for targeting software and onboard data processing. Simulated microhabitats added to a simulated borehole could be used to test any given software's ability to detect microhabitats and make appropriate decisions on sampling.

Appendix 6. Biological Features Resolution Requirements

The pixel scale requirements to identify a biological feature, whether at initial detection or subsequent analysis, depend on the number of pixels required to identify a pattern and the minimum size of the target feature. Feature identification requires having enough of a pattern to distinguish it from background noise confidently. **Figure 11** presents a graphic showing patterns composed of varying numbers of pixels and an example image of multiple features in a simulated instrument image. A single pixel (without other identifying data such as spectra or colorimetric tagging) is not sufficient to confidently distinguish it from either "hot pixel" or "cold pixel" noise. However, a pattern composed of two paired pixels will increase confidence since there is an association, and any differing alignment can be ascribed to differing orientations of that type of feature. A pattern composed of three aligned pixels provides more confidence, while a pattern composed of four or more pixels provides ever-increasing confidence that a feature has been positively detected. Identifying whether it is biological or not will require structures or patterns, providing increasing confidence that the feature is not abiotic. Features containing 2 or 3 pixels could be explained as a zonation due to inorganic chemistry.

As seen in **Figure 11**, a more complex repeating pattern with 6 pixels (5 pixels if negative space is excluded) would be more complicated to explain. However, more pixels do not guarantee unambiguous detection. The 9-pixel feature (5 pixels if negative space is excluded) in **Figure 11** could be a cell, a bubble, or a spherical zonation. Thus, the number of pixels alone is not sufficient to guarantee identification.

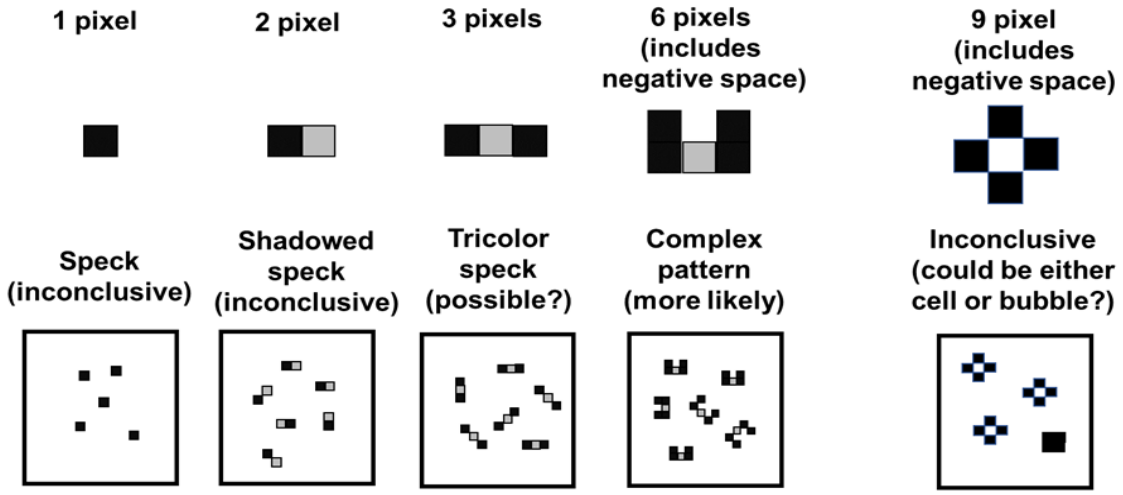

Figure 11. Graphic showing features of different pixels (upper section of graphic) and a simulated view of a collection of features of this size in varying orientations against a uniform background. The one-pixel features can be mistaken for hot (or cold) pixels. The two-pixel features show an association. Larger, more complex pixel patterns provide more confidence that the feature is real and not an artifact. However, the symmetrical feature at the far left, even though it is composed of many features, could be caused by a bubble or cell. Graphic credit: Michael J. Malaska.

Table 9 presents a compilation of various feature sizes and a subjective, estimated number of pixels required to identify that feature type. The minimum size of a biological cell was estimated in (Nealson 1997). In that work, chemical constraints based on working cellular concentrations and cellular volumes limited the estimated minimum cell size to 0.1 microns. Interestingly, in subsequent years, ultrasmall bacteria have been isolated from deep in the Greenland Ice Sheet (Miteva and Brenchley 2005) as well as ultrasmall parasitic DPANN archaea (Hamm, Erdmann et al. 2019) from extreme environments, including Antarctic hypersaline lakes that are near this size limit. If we take the minimum cell size of 0.1 microns and assume that only three pixels are required to identify it as a cell (Figure 12) positively, then a pixel scale of 0.03 microns per pixel would be sufficient. (If the number were relaxed to only requiring 2 pixels, then 0.05 microns per pixel would be adequate.)

Table 9. Minimum image scale requirements to identify a biological cell.

Type Feature	Feature size [long dimension in microns]	Estimated pixels needed for biotic/abiotic identification [long dimension]	Image scale requirement [microns per pixel]
Detailed diatom (Malaska et al., unpublished data, see Figure 12)	10	7	1.4
Sea ice bacteria (Junge et al., 2004)	3.8	10	0.4
Ultrasmall ice core bacteria (Miteva and Brenchley, 2005)	0.2	10	0.02
Theoretical minimum cell size limit (Nealson, 1997)	0.1	3	0.03

However, these are idealized estimates assuming a clear morphology. Higher resolution does not always translate to definitive identification. **Figure 12** shows two features in a shallow core extracted from a supraglacial melt pond on the Greenland Ice sheet. The ice core section was melting and filtered through a 0.2-micron frit, then examined the filtered materials with a scanning electron microscope. **Figure 12A** shows a scanning electron microscope image example of a morphologically complex diatom theca. With this specimen and at a pixel scale of 0.033 microns per pixel (see requirements in Table 1), clear distinctive features and patterns in the theca can enable almost specific identification of the type of diatom –a complex pattern such as this would likely not be able to be produced abiotically.

In contrast, another feature from the same ice core sample, shown in **Figure 12B** at a higher pixel scale (0.017 microns per pixel, a higher pixel scale than the values noted in Table 1, provides an example of a non-descript "rounded object" that could be biological or could be chemical (biopolymer-based collections), or even inorganic. Without additional clues, we cannot determine its nature. Thus, These two images serve as a cautionary tale that a higher image scale does not guarantee unambiguous cell identification. It depends on the presence and scale of distinctive features for that sample.

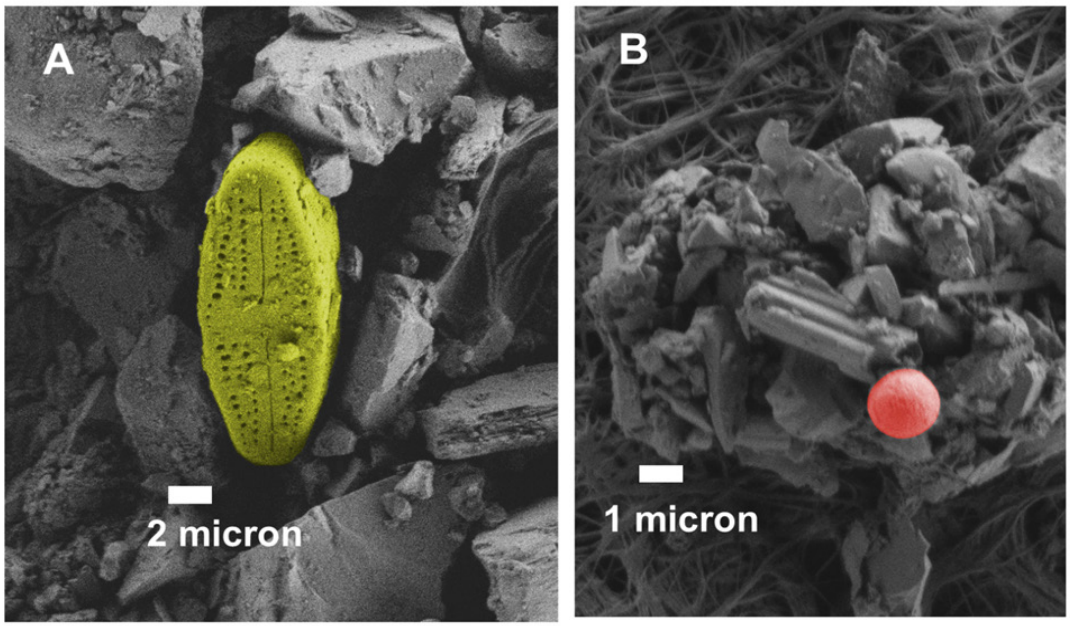

Figure 12. Scanning electron images taken from isolated filtered material from supraglacial pond ice samples. A) Colorized (yellow) Image of a diatom theca mixed with fine sediment grains. Clear indications of symmetrical puncta, rapheae, and girdle bands identify this as a diatom. Image scale is 0.033 microns per pixel. B) Image of a small rounded feature colorized in red attached to a cluster of grain materials. (deep background is of filter). The indistinct feature has no clear morphologic signature identifying it as biological, chemical, or other rounded material. Image scale is 0.017 microns per pixel. Images adapted from Malaska et al., unpublished results.

Spectral analysis or specific staining agents can be added to identify biological materials better and break these degeneracies. In the absence of specific staining agents, deep UV autofluorescence can be sufficient to discriminate based on details of the emission spectra of

features. In particular, under Deep UV excitation, some amino acids such as tryptophan, phenylalanine, tyrosine, and, to a smaller extent, histidine have distinctive fluorescent emission lambda max values (Bhartia, Salas et al. 2010). For tryptophan, the lambda max value depends on the local bulk-averaged chemical environment, so different microbes and growth stages can be differentiated based on native autofluorescence. Autofluorescent approaches have the advantage of not requiring added reagents. However, they suffer from degeneracies since abiotic organic and even inorganic materials may cause similar spectral responses. The lack of autofluorescence can be used as a negative discriminator for biology since something that is not autofluorescent is likely to be non-living. When combined with non-fluorescent imaging approaches, information on morphology and spectral characteristics can identify spots of interest.

Figure 13 shows an example of *Bacillus pumilis* cells cultured on a metal coupon. Figure 13 A shows a visible light image with only spots and features noted: some features may be cells while others may not. **Figure 13** B shows the autofluorescence centered at the tryptophan emission lambda max at 320 nm—clear blobs of higher intensity emission signal, likely bacteria. The combination of both images in **Figure 13** C shows complementary information from visible light context and autofluorescence intensity. While autofluorescence is insufficient, it can be used as a necessary initial test to aid in targeting or provide additional information for later tests.

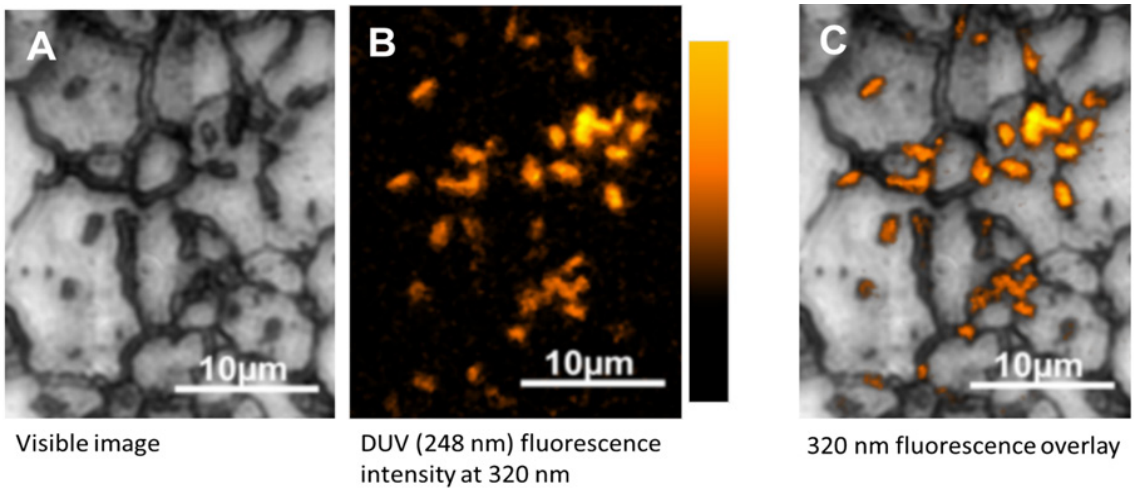

Figure 13. Autofluorescence imaging of bacteria using deep-UV excitation. A: Visible light image of *Bacillus pumilla* on a metal coupon. B: Deep UV autofluorescence imaging of the same scene. Excitation illumination is 224 nm, while fluorescence emission imaging is 320 nm. The orange coloring is proportional to signal intensity. C: image combination of visible and fluorescence imaging. Some dark spots in the visible light image correspond to fluorescence signals consistent with bacteria—figure adapted from Fig. 4 of (Bhartia, Salas et al. 2010) and used with permission of the author.

Staining agents that target certain structures, properties, or molecular functional groups can provide additional information about the target. Staining agents can be either general or specific. Examples include DAPI and BONCAT staining techniques. The fluorescing agents can bind to materials at low concentrations and positively identify biological materials such as intact cells based on a combination of staining (this material binds) and shape (this material

binds and has the correct shape.). Staining native samples requires careful technique to prevent osmotic shock that could rupture cell walls. In their work with sea ice micropockets, (Junge, Krembs et al. 2001, Junge, Eicken et al. 2004) carefully diffused in DAPI stain to allow it to penetrate the hypersaline pockets and microveins without causing bulk melting of the surrounding ice grains (**Figure 14**).

In much the same way as autofluorescence, the fluorescent features indicate cells. However, the specificity of the DAPI stain to AT-rich regions of double-stranded DNA provides even more information about the target. In an example of even more chemical specificity, (Marlow, Colocci et al. 2020) used BONCAT fluorescence staining to identify differentially metabolizing microbes coupled with scanning electron microscopy when examining fumarole microenvironments. While staining techniques are powerful, incorporating staining techniques on a flight mission for either on-board analysis or directly to the sample in an in situ instrument would be technically challenging.

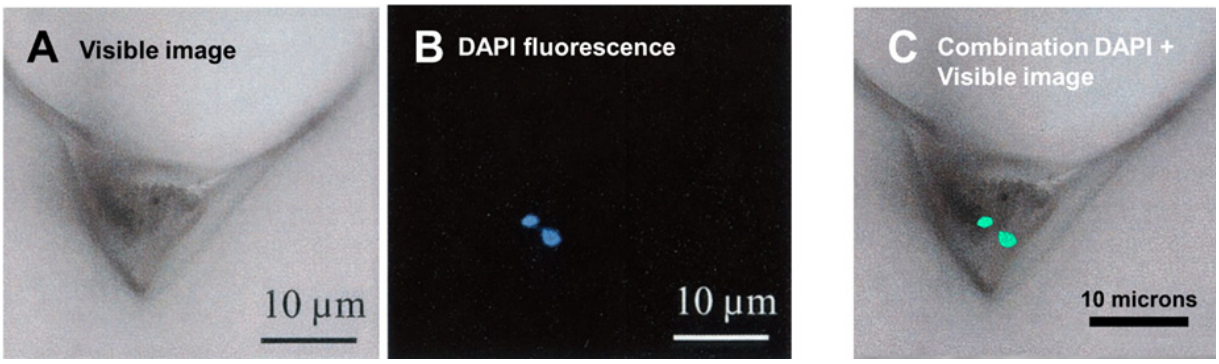

Figure 14. DAPI staining of bacteria in a sea ice micropocket using epifluorescence. **A:** Visible light image of a micropocket in a sea ice sample. **B:** DAPI staining epifluorescence imaging of the same scene. Two fluorescent spots corresponding to bacteria are observed in the micropocket. **C:** a combination of visible and fluorescence imaging. The bacteria are not visible in the visible image. Adapted from Fig 1b in (Junge, Eicken et al. 2004), Figure 1B in text and used with permission of the author.

References

(NASA), N. A. a. S. A. (2021). Mars Life Explorer: Mission Concept Study – Planetary Science and Astrobiology Decadal Survey. Washington, D.C. , National Aeronautics and Space Administration (NASA).

Affholder, A., F. Guyot, B. Sauterey, R. Ferrière and S. Mazevet (2022). "Putative methanogenic biosphere in Enceladus' deep ocean: biomass, productivity and implications for detection." The Planetary Science Journal **3**(270).

Barletta, R. W., J. C. Pricsu, H. M. Mader, W. L. Jones and C. W. Roe (2012). "Chemical analysis of ice vein μ-environments II – Analysis of glacial samples from Greenland and the Antarctic." Journal of Glaciology **58**: 1109-1118.

Berezin, M. and S. Achilefu (2010). "Fluorescence Lifetime Measurements and Biological Imaging." Chemical Reviews **110**: 2641-2684.

Bhartia, R., E. C. Salas, W. F. Hug, R. D. Reid, A. L. Lane, K. J. Edwards and K. H. Nealson (2010). "Label-free bacterial imaging with Deep-UV-laser-induced native fluorescence." Applied and Environmental Microbiology **76**: 7231-7237.

Bittel, A. M. and et al. (2018). "Varied Length Stokes Shift BODIPY-Based Fluorophores for Multicolor Microscopy." Scientific Reports **8**: 4590.

Brumwell, X., S. Kitchen and P. Zulch (2023). Optimizing Heterogeneous Platform Allocation Using Reinforcement Learning, Big Sky, MT, USA.

Burks, L., H. M. Ray, J. McGinley, S. Vunnam and N. Ahmed (2023). "HARPS: An Online POMDP Framework for Human-Assisted Robotic Planning and Sensing." IEEE Transactions on Robotics **39**(4): 3024-3042.

Carns, R. C., R. E. Brandt and S. G. Warren (2015). "Salt precipitation in sea ice and its effect on albedo, with application to Snowball Earth." Journal of Geophysical Research: Oceans **120**(11): 7400-7412.

Carstea, E. M., C. L. Popa, A. Baker and J. Bridgeman (2020). "In situ fluorescence measurements of dissolved organic matter: A review." Science of the Total Environment **699**.

Chan, M. A. and et al. (2019). "Deciphering Biosignatures in Planetary Contexts." Astrobiology **19**: 1075-1102.

Cleaves, H. J. (2012). "Prebiotic Chemistry: What We Know, What We Don't." Evolution: Education and Outreach **5**: 342-360.

Coble, P. G., R. G. M. Spencer, A. Baker and D. M. Reynolds (2014). Aquatic Organic Matter Fluorescence. New York, Cambridge University Press.

Colander, C., W. J. Bekski and M. Huber (2021). Learning the Next Best View for 3D Point Clouds via Topological Features, Xi'an, China.

Cooper, Z. S., J. Z. Rapp, S. D. Carpenter, G. Iwahana, H. Eicken and J. W. Deming (2019). "Distinctive microbial communities in subzero hypersaline brines from Arctic coastal sea ice and rarely sampled cryopegs." FEMS Microbiology Ecology **95**(12): fiz166.

Craven, M., I. Allison, H. A. Fricker and R. Warner (2009). "Properties of a marine layer under the Amery Ice Shelf, East Antarctica." Journal of Glaciology **55**: 717-728.

Dachwald, B., J. Mikucki, S. Tulaczyk, I. Digel, C. Espe, M. Feldmann, G. Francke, J. Kowalski and C. Xu (2017). "IceMole: a maneuverable probe for clean in situ analysis and sampling of subsurface ice and subglacial aquatic ecosystems." Annals of Glaciology **55**.

Dal Co, A., S. van Vliet, D. J. Kiviet, S. Schlegel and M. Ackermann (2020). "Short-range interactions govern the dynamics and functions of microbial communities." Nature Ecology & Evolution **4**(3): 366-375.

Dartnell, L. R., M. C. Storrie-Lombardi and J. M. Ward (2010). "Complete fluorescent fingerprints of extremophilic and photosynthetic microbes." International Journal of Astrobiology **9**: 245-257.

Datta, R., A. Gillette, M. Stefely and M. C. Skala (2021). "Recent innovations in fluorescence lifetime imaging microscopy for biology and medicine." Journal of Biomedical Optics **26**.

Deming, J. W. (2007). Life in ice formations at very cold temperatures. Physiology and Biochemistry of Extremophiles**:** 133-144.

Deming, J. W. (2009). Sea Ice Bacteria and Viruses. Sea Ice Second Edition. D. N. Thomas and G. S. Diekmann, Wiley.

Dundas, C. M., M. T. Mellon, L. V. Posiolova, K. Miljković, G. S. Collins, L. L. Tornabene, V. G. Rangarajan, M. P. Golombek, N. H. Warner, I. J. Daubar and S. Byrne (2023). "A large new crater exposes the limits of water ice on Mars." Geophysical Research Letters **50**(2): e2022GL100747.

Fike, D. A., D. L. Gammon, W. Ziebis and V. J. Orphan (2008). "Micron-scale mapping of sulfur cycling across the oxycline of a cyanobacterial mat: a paired nanoSIMS and CARD-FISH approach." The ISME Journal **2**: 749-759.

Fox-Powell, M. G. and C. R. Cousins (2021). "Partitioning of crystalline and amorphous phases during freezing of simulated Enceladus ocean fluids." Journal of Geophysical Research: Planets **126**(1): e2020JE006628.

Glass, B., C. Fortuin, H. Battah and I. King (2024). TRIDENT Drill Validation Testing in Haughton Crater, Devon Island, Canada. Earth and Space 2024**:** 294-300.

Glass, B., J. Heldmann, C. McKay, D. Bergman, A. Dave, A. Davila, J. Eigenbrode, V. Parro, R. Quinn and C. Stoker (2023). The Icebreaker Life Mission to Mars: A Search for Biomolecular Evidence of Recent Life. Technology Showcase for Future NASA Planetary Science Missions.

Glass, B., T. Stucky, S. Seitz, A. Dave and R. Haynes (2023). Repurposing Drilling Control Diagnostics for Subsurface Edge Detection and Boundary Advisement during Planetary Drilling. Earth and Space 2022**:** 232-242.

Glavin, D. P., A. S. Burton, J. E. Elsila, J. C. Aponte and J. P. Dworkin (2020). "The Search for Chiral Asymmetry as a Potential Biosignature in our Solar System." Chemical Reviews **120**(11): 4660-4689.

Glavin, D. P., H. L. McLain, J. P. Dworkin, E. T. Parke, J. E. Elsila, J. C. Aponte, D. M. Simkus, C. I. Pozarycki, H. V. Graham, L. R. Nittler and C. M. O. D. Alexander (2020). "Abundant extraterrestrial amino acids in the primitive CM carbonaceous chondrite Asuka 12236." Meteoritics and Planetary Science **55**: 1979-2006.

Hamm, J. N., S. Erdmann, E. A. Eloe-Fadrosh, A. Angeloni, L. Zhong, C. Brownlee, T. J. Williams, K. Barton, S. Carswell, M. A. Smith, S. Brazendale, A. M. Hancock, M. A. Allen, M. J. Raftery and

R. Cavicchioli (2019). "Unexpected host dependency of Antarctic Nanohaloarchaeota." Proceedings of the National Academies of Sciences **116**: 14661-14670.

Hand, K. P., A. E. Murray, J. N. Garvin, W. B. Brinckerhoff, B. C. Christner, K. S. Edgett, B. L. Ehlmann, C. R. German, A. G. Hayes, T. M. Hoehler, S. M. Horst, J. I. Lunine, K. H. Nealson, C. Paranicas, B. E. Schmidt, D. E. Smith, A. R. Rhoden, M. J. Russell, A. S. Templeton, P. A. Willis, R. A. Yingst, C. B. Phillips, M. L. Cable, K. L. Craft, A. E. Hofmann, T. A. Nordheim and R. T. Pappalardo (2016). "Report of the Europa Lander Science Definition Team." NASA Report.

Huang, C. and et al. (2023). "Self-Supervised Attentive Generative Adversarial Networks for Video Anomaly Detection." IEEE Transactions on Neural Networks and Learning Systems **34**(11): 9389-9403.

Inagaki, F., K. U. Hinrichs, Y. Kubo, M. W. Bowles, V. B. Heuer, W. L. Hong, T. Hoshino, A. Ijiri, H. Imachi, M. Ito and M. Kaneko (2015). "Exploring deep microbial life in coal-bearing sediment down to ~2.5 km below the ocean floor." Science **349**(6246): 420-424.

Jayaraman, D. and K. Grauman (2018). Learning to Look Around: Intelligently Exploring Unseen Environments for Unknown Tasks, Salt Lake City, UT, USA.

Junge, K., H. Eicken and J. W. Deming (2004). "Bacterial activity at -2 to -20 °C in Arctic wintertime sea ice." Applied and Environmental Microbiology **70**(1): 550-557.

Junge, K., C. Krembs, J. Deming, A. Stierle and H. Eicken (2001). "A microscopic approach to investigate bacteria under in situ conditions in sea-ice samples." Annals of Glaciology **33**: 304-310.

Khuller, A. R., L. Kerber, M. E. Schwamb, S. Beer, F. E. Nogal, R. Perry and C. J. Hansen (2023). "Irregular Polygonal Ridge Networks in Arabia Terra, Nili Fossae and Nilosyrtis." The Dynamics & Evolution of Martian Ices: Implications for Present-Day Liquid Water **203**.

Koga, T. and H. Naraoka (2017). "A new family of extraterrestrial amino acids in the Murchison meteorite." Scientific Reports **7**: 636.

Lee, P., S. Shubham and J. Schutt (2023). A relict glacier near Mars' equator: Evidence for recent glaciation and volcanism in Eastern Noctis Labyrinthus.

Lewis, E. L. and R. G. Perkin (1986). "Ice pumps and their rates." Journal of Geophysical Research: Oceans **91**(C10): 11756-11762.

Li, K. and et al. (2022). "Spectral-Spatial Deep Support Vector Data Description for Hyperspectral Anomaly Detection." IEEE Transactions on Geoscience and Remote Sensing **60**: 1-16.

Ma, N., M. A. Digman, L. Malacrida and E. Gratton (2016). "Measurements of absolute concentrations of NADH in cells using the phasor FLIM method." Biomed Opt Express **7**(7): 2441-2452.

MacKenzie, S. M., M. Neveu, A. F. Davila, J. I. Lunine, K. L. Craft, M. L. Cable, C. M. Phillips-Lander, J. D. Hofgartner, J. L. Eigenbrode, J. H. Waite and C. R. Glein (2021). "The Enceladus Orbilander mission concept: Balancing return and resources in the search for life." The Planetary Science Journal **2**(2): 77.

Mader, H. M., M. E. Pettitt, J. Wadham, E. W. Wolff and R. J. Parkes (2006). "Subsurface ice as a microbial habitat." Geology **34**: 169-172.

Malaska, M. J., R. Bhartia, K. S. Manatt, J. C. Priscu, W. J. Abbey, B. Mellerowicz, J. Palmowski, G. L. Paulsen, K. Zacny, E. J. Eshelman and J. D'Andrilli (2020). "Subsurface in situ detection of

microbes and diverse organic matter hotspots in the Greenland ice sheet." Astrobiology **20**: 1185-1211.

Marlow, J., R. Spietz, K.-Y. Kim, M. Ellisman, P. Girguis and R. Hatzenpichler (2021). "Spatially resolved correlative microscopy and microbial identification reveal dynamic depth- and mineral-dependent anabolic activity in salt marsh sediment." Environmental Microbiology **23**(8): 4756-4777.

Marlow, J. J., I. Colocci, S. P. Jungbluth, N. M. Weber, A. Gartman and J. Kallmeyer (2020). "Mapping metabolic activity at single cell resolution in intact volcanic fumarole sediment." FEMS Microbiology Letters **367**(1).

Miteva, V. I. and J. E. Brenchley (2005). "Detection and isolation of ultrasmall microorganisms from a 120,000-year-old Greenland glacier ice core." Applied and Environmental Microbiology **71**(12): 7806-7818.

Nealson, K. H. (1997). "The limits of life on Earth and searching for life on Mars." Journal of Geophysical Research **102**: 23675-23686.

Neish, C., M. J. Malaska, C. Sotin, R. M. C. Lopes, C. A. Nixon, A. Affholder, A. Chatain, C. Cockett, K. K. Farnsworth, P. M. Higgins, K. E. Miller and K. M. Soderland (2024). "Organic input to Titan's subsurface ocean through impact cratering." Astrobiology **24**(177).

Obreht, I., L. Wörmer, A. Brauer, J. Wendt, S. Alfken, D. De Vleeschouwer, M. Elvert and K. U. Hinrichs (2020). "An annually resolved record of Western European vegetation response to Younger Dryas cooling." Quaternary Science Reviews **231**: 106198.

Ojha, L., M. B. Wilhelm, S. L. Murchie, A. S. McEwen, J. J. Wray, J. Hanley and M. Chojnacki (2015). "Spectral evidence for hydrated salts in recurring slope lineae on Mars." Nature Geoscience **8**(11): 829-832.

Pizzarello, S., D. L. Schrader, A. A. Monroe and D. S. Lauretta (2012). "Large enantiomeric excesses in primitive meteorites and the diverse effects of water in cosmochemical evolution." Proceedings of the National Academy of Sciences **109**: 11949-11954.

Price, P. B. (2000). "A habitat for psychrophiles in deep Antarctic ice." Proceedings of the National Academy of Sciences **97**: 1247-1251.

Priscu, J. and K. O. Hand (2012). "The microbial habitability of extraterrestrial icy worlds: A view from Earth." Microbe **7**: 167-172.

Rafeek, S., S. Gorevan, P. Bartlett and K. Kong (2001). The inchworm deep drilling system for kilometer scale subsurface exploration of Europa (IDDS). Forum on Innovative Approaches to Outer Planetary Exploration 2001-2020.

Rapp, J. Z., M. B. Sullivan and J. W. Deming (2021). "Divergent genomic adaptations in the microbiomes of Arctic subzero sea-ice and cryopeg brines." Frontiers in Microbiology **12**: 701186.

Ravier, R., D. Garagić, J. Peskoe, T. Galoppo, J. Tigue, B. J. Rhodes and P. Zulch (2023). Online Reinforcement Learning for Autonomous Sensor Control. 2023 IEEE Aerospace Conference.

Rohde, R. A. (2010). "The development and use of the Berkeley fluorescence spectrometer to characterize microbial content and detect volcanic ash in glacial ice." Ph.D. Thesis, University of California at Berkeley.

Roldan, M., C. Ascaso and J. Wierzchos (2014). "Fluorescent fingerprints of endolithic phototrophic cyanobacteria living within halite rocks in the Atacama Desert." Applied and Environmental Microbiology **80**: 2998-3006.

Sattler, B., M. C. Storrie-Lombardi, C. M. Foreman, M. Tilg and R. Psenner (2010). "Laser-induced fluorescence emission (LIFE) from Lake Fryxell (Antarctica) cryoconites." Annals of glaciology **51**(56): 145-152.

Shi, H., W. Mao, Y. Zhang and X. Liang (2023). "Unsupervised deep tensor multitask anomaly detection with rule adaptation for online early fault evaluation." IEEE Sensors Journal **23**(8): 8665-8679.

Shkolyar, S., E. J. Eshelman, J. D. Farmer, D. Hamilton, M. G. Daly and C. Youngbull (2018). "Detecting kerogen as a biosignature using colocated UV time-gated Raman and fluorescence spectroscopy." Astrobiology **18**(4): 431-453.

Smriga, S., D. Ciccarese and A. R. Babbin (2021). "Denitrifying bacteria respond to and shape microscale gradients within particulate matrices." Communications Biology **4**(1): 570.

Van Der Wielen, P. W., H. Bolhuis, S. Borin, D. Daffonchio, C. Corselli, L. Giuliano, G. D'Auria, G. J. De Lange, A. Huebner and S. P. Varnavas (2005). "The enigma of prokaryotic life in deep hypersaline anoxic basins." Science **307**(5706): 121-123.

van Gestel, J., T. Bareia, B. Tenennbaum, A. Dal Co, P. Guler, N. Aframian, S. Puyesky, I. Grinberg, G. G. D'Souza, Z. Erez, M. Ackermann and A. Eldar (2021). "Short-range quorum sensing controls horizontal gene transfer at micron scale in bacterial communities." Nature Communications **12**(1): 2324.

van Tatenhove-Pel, R. J., T. Rijavec, A. Lapanje, I. van Swam, E. Zwering, J. A. Hernandez-Valdes, O. P. Kuipers, C. Picioreanu, B. Teusink and H. Bachmann (2020). "Microbial competition reduces metabolic interaction distances to the low µm-range." The ISME Journal **15**(3): 688-701.

Vance, S. D., M. P. Panning, S. Stähler, F. Cammarano, B. G. Bills, G. Tobie, S. Kamata, S. Kedar, C. Sotin, W. T. Pike, R. Lorenz, H.-H. Huang, J. M. Jackson and B. Banerdt (2018). "Geophysical Investigations of Habitability in Ice-Covered Ocean Worlds." Journal of Geophysical Research: Planets **123**(1): 180-205.

Winebrenner, D. P., J. Burnett, B. Brand, W. T. Elam, S. Wensman, R. C. Bay, M. Pickett and S. Tyler (2024). "Successes and Challenges in Realizing an Instrumented Ice Melt Probe to Reach Kilometer Depths in Antarctica Within a Single Field Season." AGU24.

Winebrenner, D. P., W. T. Elam, P. M. Kintner, S. Tyler and J. S. Selker (2016). Clean, logistically light access to explore the closest places on Earth to Europa and Enceladus. AGU Fall Meeting Abstracts.

Wolfenbarger, N. S., J. J. Buffo, K. M. Soderlund and D. D. Blankenship (2022). "Ice shell structure and composition of ocean worlds: insights from accreted ice on Earth." Astrobiology **22**(8): 937-961.

Yang, W. and S. L. Chen (2020). "Time-gated fluorescence imaging: Advances in technology and biological applications." Journal of Innovative Optical Health Sciences **13**: 2030006.

Zimmerman, W., R. Bonitz and J. Feldman (2001). Cryobot: an ice penetrating robotic vehicle for Mars and Europa, Big Sky, MT, USA.


Keck
INSTITUTE FOR SPACE STUDIES